AN ABSTRACT OF THE THESIS OF

Richard Clark Landgraf for the Master of Science in Electrical
(Name) (Degree) (Major)

Engineering

Date thesis is presented June 26, 1964

Title SIGNAL TRANSFER AND GAIN IN MAGNETIC-CORE CIRCUITS

Abstract approved [redacted]
(Major professor)

Because of its characteristics, the square-loop magnetic core can be used as the basic device in a logic system. A magnetomotive force (mmf) which is below the threshold mmf of such a core will cause a negligible, nonpermanent amount of flux change in the core; and information signals can be distinguished by the amount of flux change they produce in the core. The remanent flux in a magnetic core can be in the clockwise or counterclockwise direction, and the binary information signals ONE and ZERO can be represented by these two directions of flux.

The transfer of information in a logic system will introduce noise and cause losses, and the ability of the circuits in a system to respond properly to degraded signals will be determined largely by the transfer characteristics of the circuits. The transfer process is shown to be basically identical for three examples of magnetic-core shift registers, and it is shown that there must be an imbalance of the number of turns on the windings in the coupling loop between a

transmitting and a receiving core. For economic reasons this winding imbalance is undesirable, and a circuit requiring only single-turn windings in the coupling loop is proposed. An experimental investigation of the proposed circuit showed that its transfer characteristics are determined by the resistance and inductance in the coupling loop and the amplitude of the current pulse driving the circuit. Voltage waveforms of the circuit seem to indicate that the inductance, which is normally assumed to be detrimental to the circuit operation, might have an optimum value which would be beneficial to the transfer process.

SIGNAL TRANSFER AND GAIN IN MAGNETIC-CORE CIRCUITS

by

RICHARD CLARK LANDGRAF

A THESIS

submitted to

OREGON STATE UNIVERSITY

in partial fulfillment of
the requirements for the
degree of

MASTER OF SCIENCE

June 1965

APPROVED: [redacted]

Professor of Electrical Engineering and Head of Electrical Engineering Department

In Charge of Major

[redacted]

Dean of Graduate School

Date thesis is presented June 26, 1964

Typed by Opal Grossnicklaus

ACKNOWLEDGMENT

The author wishes to thank Professor L. N. Stone of the Electrical Engineering Department for his help and continued interest in this work. Criticism of the thesis by Professor R. L. Krahmer was appreciated.

TABLE OF CONTENTS

LIST OF ILLUSTRATIONS

TABLE

SIGNAL TRANSFER AND GAIN IN MAGNETIC-CORE CIRCUITS

INTRODUCTION

The square-loop ferrite toroid, so-called because of the shape of its hysteresis characteristic, has been investigated by many people with the intention of using it as the basic element in a logic system. One of the reasons motivating these investigations has been the possibility of realizing a logic system almost devoid of semiconductor devices. This is desirable because it appears that a system composed only of wire and ferrite toroids is potentially more reliable than a system utilizing many semiconductors. Another reason for the attractiveness of a ferrite logic system is its immunity to damage by particle (or nuclear) radiation. The importance of this consideration is attested to by some earth-satellite failures which have been attributed to semiconductor degradation as a result of exposure to particle (or nuclear) radiation in space.

The majority of the existing logic systems operate on a binary basis. The reason for this is that with the devices available it is most convenient to arrange circuits so that they have two easily distinguishable states. For instance, a transistor circuit might be said to be in the ONE or ZERO logic condition depending on whether the

collector voltage of the transistor is at a high level or a low level. The same logic conditions in a ferrite toroid might correspond to remanent flux in the clockwise or counterclockwise direction.

For a system to be useful, the logic condition of one circuit must be capable of influencing the condition of another circuit. In other words, a means must be provided to transfer logic conditions or signals between individual circuits. It is inevitable in a physical system that there will be some loss and noise introduced in the transfer process; thus, a circuit must be capable of making the proper response even though the input to it might be less than a ONE or greater than a ZERO. In terms of amplification, this specifies that for signals close to ONE the logic circuit must have a gain greater than one; and when the signals are close to ZERO, the gain must be less than one. If the transfer network between two magnetic-core circuits is considered in relation to the flux levels in the cores involved, then an expression for gain may be derived in terms of the flux levels. Thus, a magnetic-core circuit may be considered as a flux amplifier. Because magnetic cores have extremely nonlinear characteristics, circuits using them cannot be readily analyzed mathematically. Therefore, the effects of the transfer-network parameters and power source on the transfer process must be derived experimentally.

CORE CHARACTERISTICS

The reasons for considering a ferrite toroid for use as a logic element are apparent from a consideration of the flux versus magnetomotive force (mmf) characteristic. An idealized version of this characteristic is shown in Fig. 1. With no mmf applied, the flux in a core can have any value between $-\phi_r$ and $+\phi_r$. If a very large, negative mmf is applied to the core and then removed, the flux in the core will assume a value of $-\phi_r$. If the core now is subjected to a positive mmf of NI_1 or less, the flux in the core will be changed very little; and upon removal of the mmf, the flux level will fall to very nearly $-\phi_r$. The flux changes encountered in this operation are termed elastic changes. If an mmf of NI_2 is applied, the flux will assume a level of ϕ_2. When this mmf is removed, the flux level will decrease a small amount to ϕ_2'. If an mmf of NI_3 or greater had been applied, the flux level would have become somewhat greater than $+\phi_r$; and upon removal of the mmf the flux would have fallen to $+\phi_r$.

Thus, the core described by Fig. 1 has two stable, easily distinguishable states, namely $+\phi_r$ and $-\phi_r$. The core has memory because when it is subjected to an mmf of NI_3 or greater, the core retains this information by remaining at $+\phi_r$ after removal of the mmf. The core has a threshold characteristic; that is, the mmf must be greater than a certain amount before any appreciable change in flux

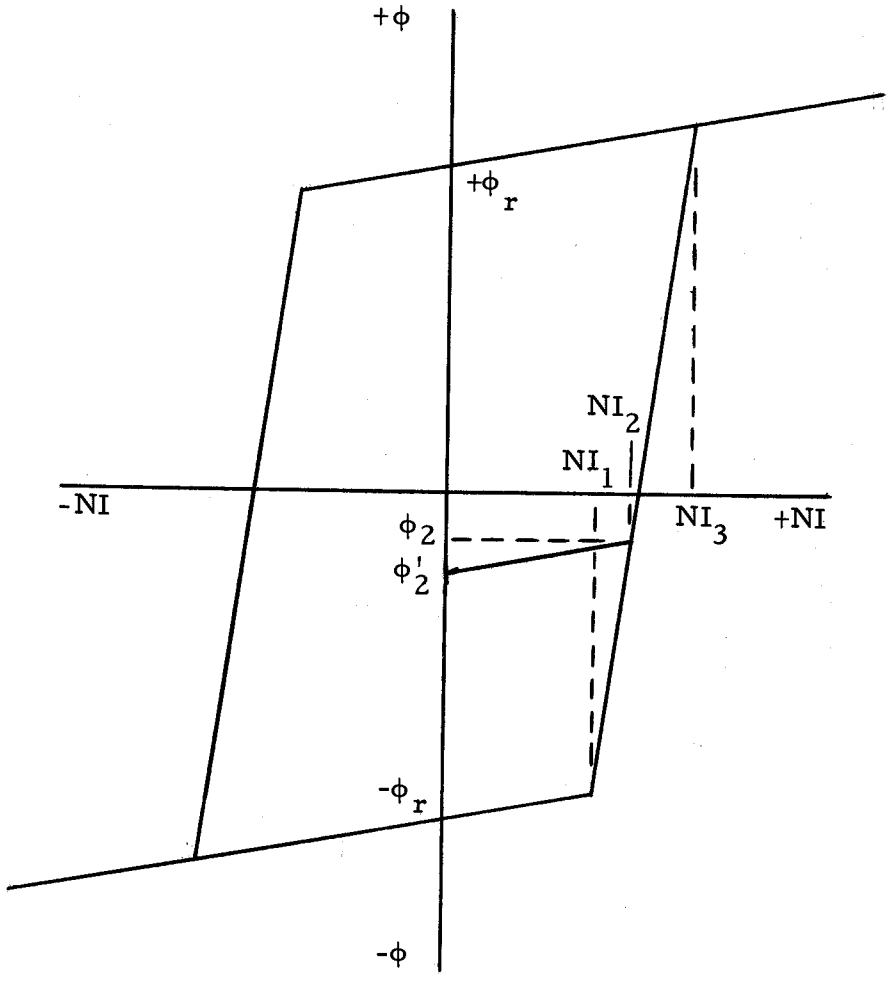

Fig. 1. Idealized flux-mmf characteristic of a magnetic core.

level takes place. This provides immunity to noise and also provides logic capability. For example, if a core has two N-turn windings on it and a current of I_1 flows in either winding but not both, there will be no change in the flux level in the core. However, if a current of I_1 flows in both windings, the mmf applied to the core will be $2NI_1$; and the flux level in the core will be changed from $-\phi_r$ to $+\phi_r$ (if $2NI_1 > NI_3$). Thus the core will perform the AND logic function. If the currents in the two windings had a magnitude of I_3, the OR function would have been realized because the presence of either one or the other or both currents would cause the flux to become $+\phi_r$.

The plot of reciprocal switching time versus applied mmf in Fig. 3 can be obtained from the circuit and waveforms shown in Fig. 2. A current pulse of the proper polarity and magnitude applied to the reset winding in Fig. 2 will establish a flux level of $-\phi_r$ in the counterclockwise direction in the core. The subsequent application of the current I will cause the flux to reverse and assume a level of $+\phi_r$ in the clockwise direction, and a voltage e will be induced in the output winding of the core. The switching time t_s is measured between the $0.1e_{max}$ points on the rising and falling portions of the voltage waveform.

The effects of varying the mmf applied to a core are shown in Fig. 3 and 4. At low values of applied mmf the switching characteristic shown in Fig. 3 is not linear. This nonlinearity seemingly

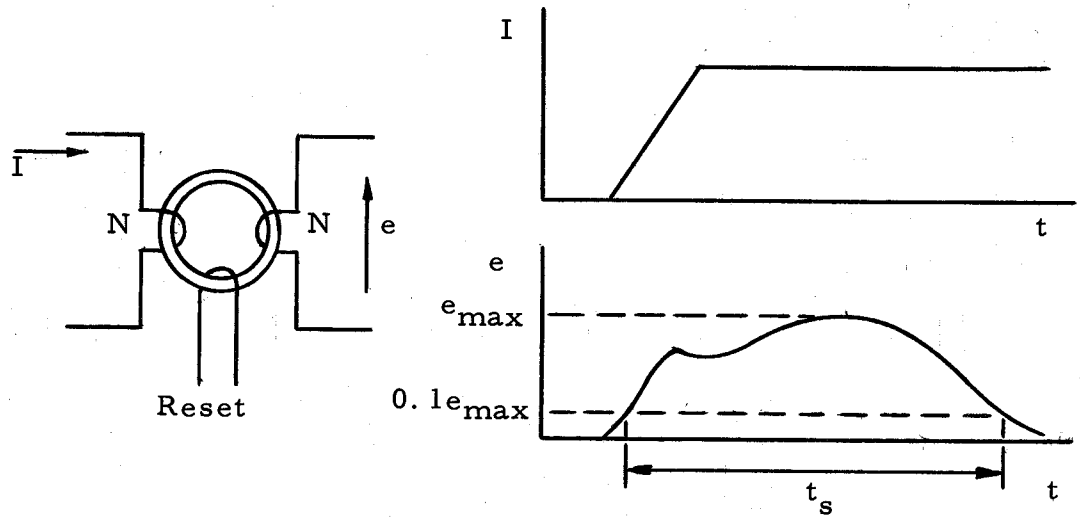

Fig. 2. Measurement of switching time t_s of a magnetic core.

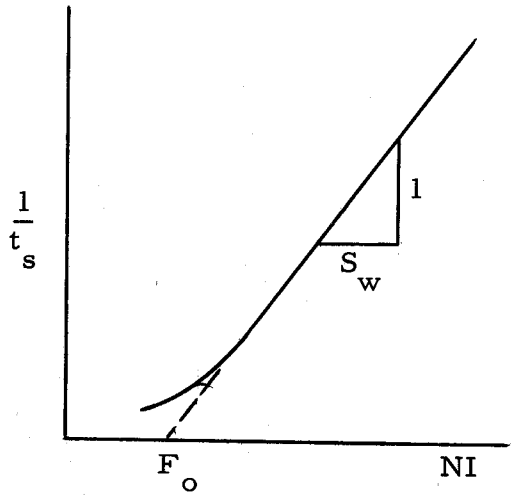

Fig. 3. Switching characteristic of a magnetic core.

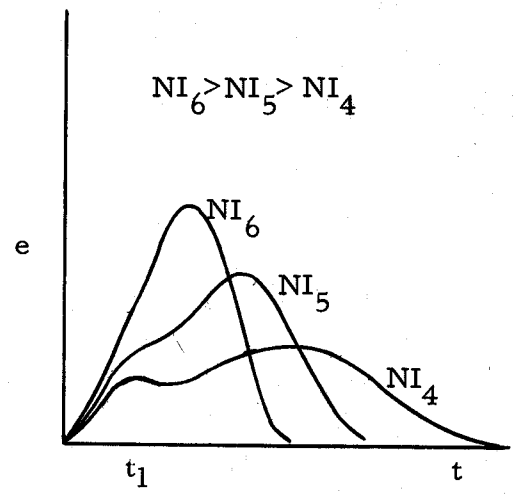

Fig. 4. Variations of the voltage waveform of a magnetic core caused by different magnitudes of mmf.

results because the flux-mmf characteristic (see Fig. 1) has a finite slope between NI_1 and NI_3. At higher values of mmf the switching characteristic is a straight line. The threshold mmf of a core is normally taken as the value at the intersection of the extrapolation of the linear portion of the curve and mmf axis. The curve shown in Fig. 3 indicates also that as the mmf increases beyond F_o, the time required to reverse the flux in the core decreases. The effect of increasing mmf on the waveshape of the output voltage is shown in Fig. 4. The values of mmf in Fig. 4 are greater than the mmf NI_3 shown in Fig. 1. As the switching time decreases, the amplitude of the output voltage increases. This results because the amount of flux change in the core is nearly constant. The voltage e induced in the N-turn winding by a change of flux ϕ in the core in Fig. 2 is

$$e = N\frac{d\phi}{dt} \tag{1}$$

Because the flux is changed from $-\phi_r$ to $+\phi_r$, the integration of equation (1) yields

$$\int e\,dt = N(2\phi_r) \tag{2}$$

Therefore, the area under the voltage waveform is constant; and the amplitude of the waveform must increase as width decreases. A measure of switching time of the core is the switching coefficient S_w, which is the inverse of the slope of the curve shown in Fig. 3.

The switching mechanism of a core as described by Menyuk

and Goodenough (8) involves reversible domain-wall motion, nucleation of domains of reverse magnetization, and irreversible domain-wall motion. A domain is a region within a core which has a uniform direction of magnetization, and a domain wall is the boundary between two such regions which have different directions of magnetization. If a core is driven into saturation ($NI > NI_3$ in Fig. 1), domains within the core will be nominally aligned in one direction; but because core material is not homogeneous, there will be local variations in the direction of magnetization. Application of a large mmf in the opposite direction will initially cause reversible domain-wall motion and nucleation of domains of reverse magnetization. The term reversible wall motion indicates that upon removal of the mmf, a domain wall that had undergone reversible motion would return to its original position. Reversible domain-wall motion and domain nucleation apparently take place within the rise time of the applied mmf. Also during the rise time of the mmf, irreversible wall motions are accelerated to an average velocity which is a function of the final value of the applied mmf. Irreversible wall motion causes the size of domains of reverse magnetization to increase. Increasing the mmf applied to the core will increase wall velocity and therefore cause the size of the reverse domains to increase faster. This results in decreased switching time with increased mmf. The minor peak indicated at time t_1 in Fig. 4 is caused by reversible wall motion and domain

creation. As the mmf is increased, this minor peak becomes obscured by the major peak.

MAGNETIC-CORE SHIFT REGISTERS

Logic circuits employing magnetic cores should be capable of transferring information, which is represented by the level of flux in a core, with minimum attenuation. The transfer problem can be introduced by examining the operation of magnetic-core shift registers. Three examples of shift-register circuits will be presented: semiconductor diodes are used in one of the circuits, and in the other circuits the functions of the diodes are performed by additional cores.

Core-Diode Circuit

One of the earliest successfully operated core shift registers was described by Wang and Woo (10). This circuit is shown in Fig. 5. A ONE logic signal or information signal is represented by a clockwise direction of flux and a ZERO by a counterclockwise direction. It will be assumed that initially core C_1 is in the ONE state and all other cores are in the ZERO state. Drive current pulses occur alternately as shown in Fig. 5. When current pulse I_a occurs, core C_1 will be set in the ZERO state. Because the other cores to which current pulse I_a is applied are in the ZERO state, flux changes within them will be negligible. Setting core C_1 to ZERO will cause a flux change of $2\phi_r$, and a voltage will be induced in winding N_2 on that core. The voltage across winding N_2 (upper terminal positive) will

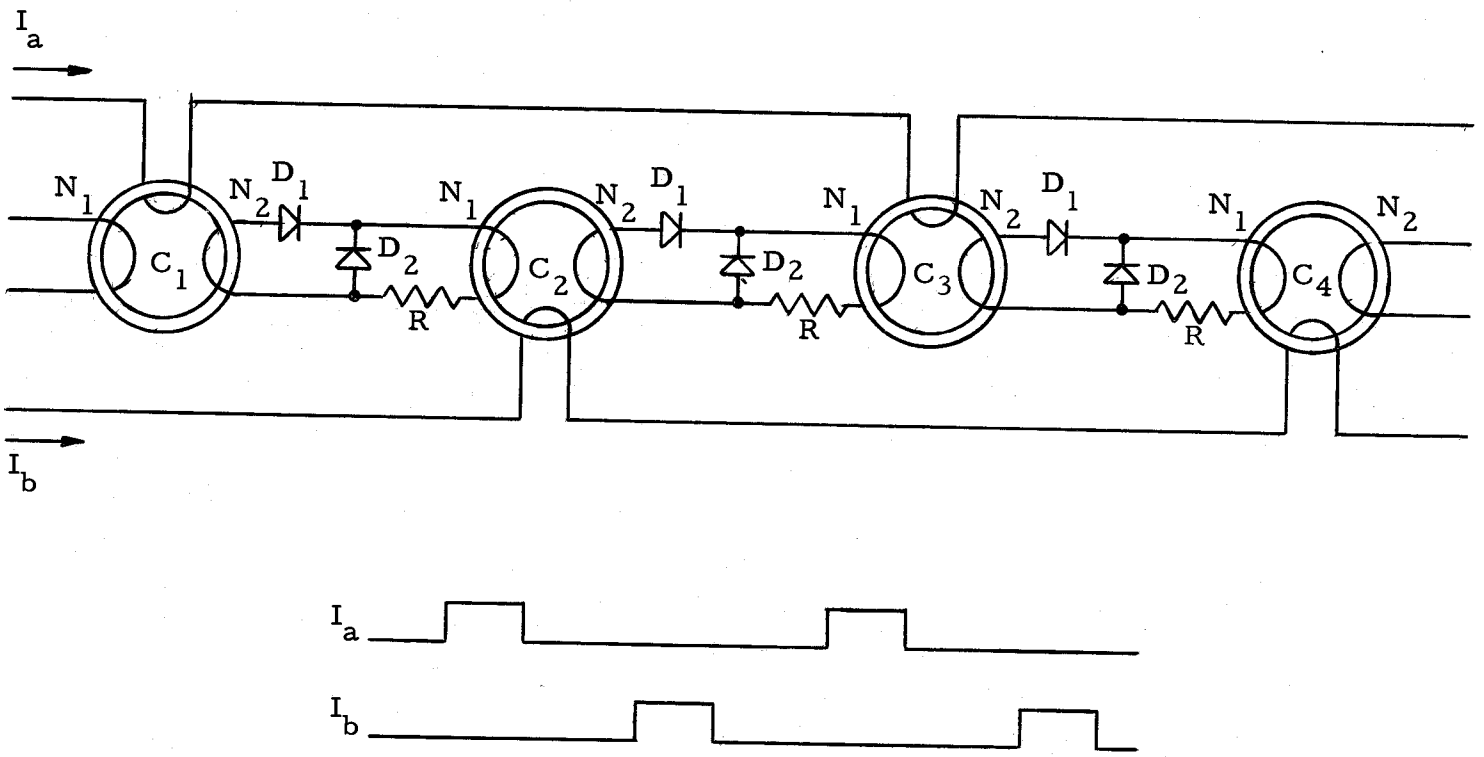

Fig. 5. Core-diode shift register.

cause a current in the coupling loop. If this current exceeds the threshold of core C_2, it will cause the flux in C_2 to switch in the clockwise direction or toward the ONE state. Because of the switching of C_2, a voltage will be induced in winding N_2 of that core with the bottom terminal of the winding positive. This voltage will reverse-bias diode D_1 in the second coupling loop, and no current will flow in that coupling loop.

If diode D_1 in each coupling loop was replaced by a short circuit, the voltage induced in winding N_2 on core C_2 would cause a current to flow in the second coupling loop. This current would cause an mmf on core C_2, and this mmf would oppose the mmf produced by the current in the first coupling loop. Therefore, the net mmf available to switch core C_2 would be reduced; and the switching time of that core would be increased. This might cause the switching time of core C_2 to be increased beyond the switching time of core C_1, and it would be impossible to set core C_2 to the full ONE state. Therefore, inclusion of diode D_1 in each coupling loop prevents an increase of switching time of a core that is being switched by a previous core.

Core C_1 has now been set to the ZERO state and core C_2 has been set to the ONE state. When current pulse I_b occurs, core C_2 will be set to the ZERO state. Core C_3 will be set to the ONE state in the same way that core C_2 was set to the ONE state when current

pulse I_a occurred. The changing flux in core C_2 will induce a voltage in winding N_1, and the bottom terminal of that winding will be positive. This voltage will forward-bias diodes D_1 and D_2 in the first coupling loop, and a portion of the loop current will flow in each of the branches. The ratio of the equivalent resistance of winding N_2 in series with diode D_1 to the equivalent resistance of diode D_2 is such that the current flowing in winding N_2 will produce an mmf on core C_1 which is less than the threshold mmf of that core. It is necessary to limit the current in winding N_2 because this current tends to set core C_1 to the ONE state. The setting of core C_1 to the ONE state by core C_2 constitutes back-transfer of information and should be avoided.

An equation for flux levels in the cores involved in the transfer of a ONE can be obtained by integrating the voltage equation of the coupling loop. During the transfer of a ONE from core C_1 to core C_2, in the circuit in Fig. 5, the voltage equation of the first coupling loop is

$$N_2 \frac{d\phi_1}{dt} = Ri + V_1 + N_1 \frac{d\phi_2}{dt} \qquad (3)$$

In equation (3), ϕ_1 and ϕ_2 are the flux levels in cores C_1 and C_2 respectively, i is the coupling-loop current, V_1 is the voltage on diode D_1, N_1 and N_2 are the number of turns on windings N_1 and N_2, R is the coupling-loop resistance, and t is time. Integrating equation

(3) over the switching time of core C_1 yields

$$N_2\phi_1 = \int(Ri + V_1)dt + N_1\phi_2 \qquad (4)$$

If the information being transferred is maintained at the maximum ONE level, the flux change in both core C_1 and core C_2 will be $2\phi_r$ (see Fig. 1); and equation (4) can then be rewritten.

$$2\phi_r(N_2-N_1) = \int(Ri + V_1)dt \qquad (5)$$

Because the term on the right in equation (5) is necessarily greater than zero, the number of turns on winding N_2 must be greater than the number of turns on winding N_1.

Resistive Coupling Loop

The circuit shown in Fig. 6, which is an example of a magnetic core circuit with a resistive coupling loop, was first described by Russell (9). It will be assumed that initially the flux in core S_1 is set in the clockwise direction (ONE), and flux in each of the other cores is set in the counterclockwise direction (ZERO). When current pulse I_a occurs, it will hold cores C_1, C_3 and S_3 in the ZERO state; and the condition of core S_1 will be changed from the ONE state to the ZERO state. A voltage will be induced in winding N_s on core S_1 (right terminal positive) causing a current in the coupling loop which will set core C_2 to the ONE state. The switching of flux in core C_2 will induce a voltage in winding N_o (bottom terminal positive) of that

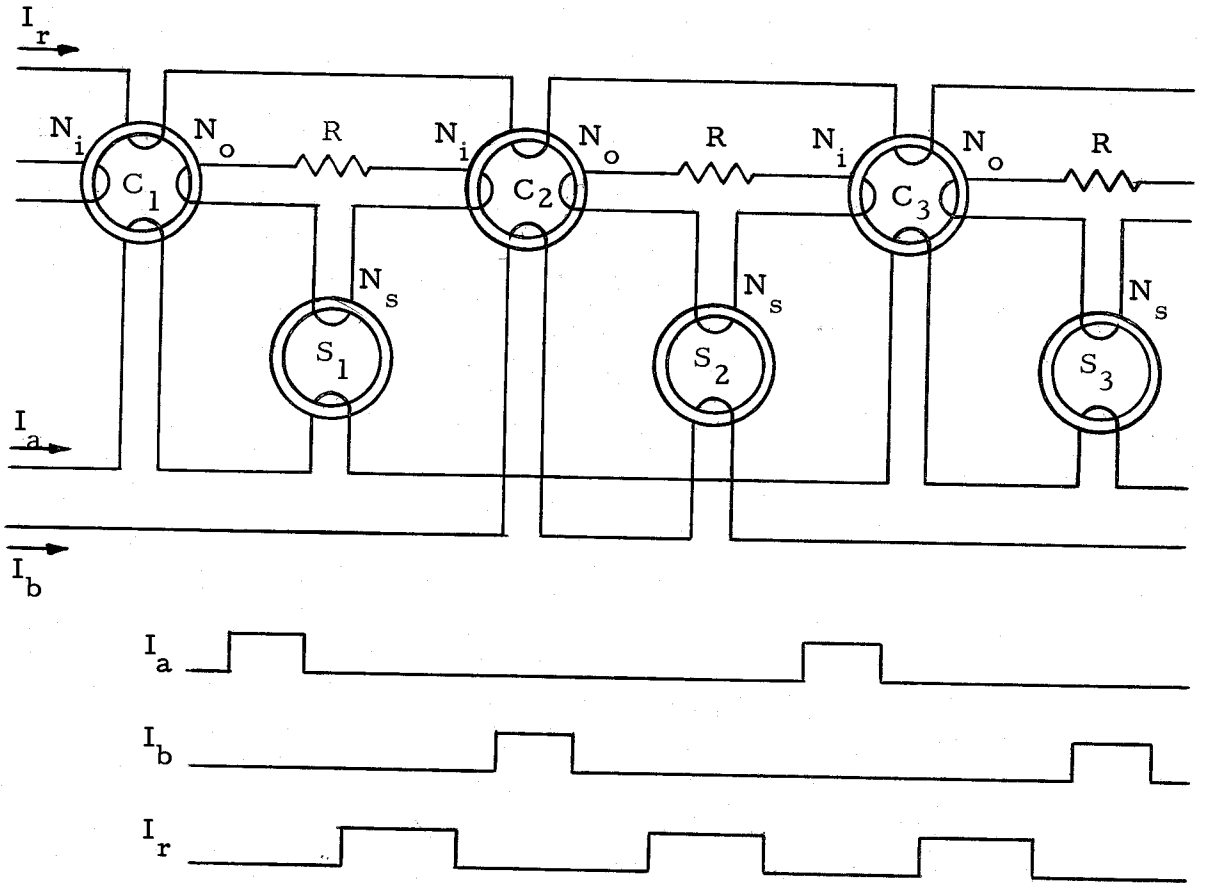

Fig. 6. Magnetic-core shift register with resistance in the coupling loop.

core, and this will cause a current to flow in the second coupling loop which will set core S_2 to the ONE state; and if it was not for current pulse I_a holding core C_3 in the ZERO state, core C_3 also would be switched to the ONE state. Thus current pulse I_a has caused core S_1 to be set to ZERO and cores C_2 and S_2 to be set to ONE. To show the function of the C cores, it will be assumed that current pulse I_r does not occur before current pulse I_b. In this case both cores S_2 and C_2 would be set to the ZERO state by current pulse I_b. The switching of core C_2 would cause a current in the first coupling loop in such a direction that core S_1 would be set to the ONE state. Thus, the ONE originally transferred from core S_1 to core S_2 would be transferred back to core S_1. Use of current pulse I_r prevents back-transfer by taking advantage of the characteristics shown in Fig. 3 and 4. If the mmf produced by current pulse I_r is limited to some value just slightly greater than the threshold of core C_2, the voltages induced in windings N_i and N_o will be small; and, consequently, the currents in the first and second coupling loops will be small. The mmf on cores S_1 and S_2 produced by these coupling-loop currents must be less than the threshold mmf of the cores. Now when current pulse I_b occurs, core C_2 will be held in the ZERO state; and, therefore, no voltage will be induced in winding N_i. Current pulse I_b will set core S_2 to the ZERO state, and cores C_3 and S_3 will be set to the ONE state in the same manner as described for cores C_2 and

S_2. The circuit shown in Fig. 6 can be analyzed in the same way that the core-diode circuit was analyzed. Voltage equations must be written for the two coupling loops involved. Because only elastic flux changes take place in cores C_1 and C_3, voltages induced in windings on these cores will be small and can be neglected. The voltage equations for the first and second coupling loops respectively are

$$N_s \frac{d\phi_{s1}}{dt} = Ri_1 + N_i \frac{d\phi_{c2}}{dt} \tag{6}$$

$$N_o \frac{d\phi_{c2}}{dt} = Ri_2 + N_s \frac{d\phi_{s2}}{dt} \tag{7}$$

Where ϕ_{s1}, ϕ_{c2}, and ϕ_{s2} represent the flux levels in cores S_1, C_2, and S_2; and i_1 and i_2 represent the currents in the first and second coupling loop respectively. These two equations can be integrated as was done with equation (3) for the core-diode circuit. If information is maintained at the maximum ONE level, the flux change in each of the three cores will be $2\phi_r$. The equations for the first and second coupling loop become respectively

$$2\phi_r(N_s - N_i) = R\int i_1 dt \tag{8}$$

$$2\phi_r(N_o - N_s) = R\int i_2 dt \tag{9}$$

Equations (8) and (9) indicate that the number of turns on the coupling loop windings must satisfy the following inequality:

$$N_o > N_s > N_i \tag{10}$$

There are limitations on switching times of cores involved in the

transfer process of the circuit shown in Fig. 6. Winding N_s on core S_1 can be considered as a source, and the energy required to switch flux in core C_2 and supply the coupling loop losses must come from this source. The switching of a core takes a finite amount of time; and to switch core C_2 completely, the voltage induced in winding N_s in the first coupling loop must persist at least as long as the switching time of core C_2. A similar argument will lead to the conclusion that the switching times of cores C_2 and S_2 must be equal. But these conditions on switching times still do not meet the requirements of the circuit. Because the voltage waveform induced in winding N_s on core S_1 will have a finite rise time, the current waveform in the coupling loop will also have a finite rise time. Core C_2 will not begin to switch until the mmf produced on that core by the current in the first coupling loop exceeds the threshold mmf of that core. Therefore, the switching time of core S_1 must be definitely longer than the switching time of core C_2. Again, the same remarks will hold for the second coupling loop and cores C_2 and S_2. To allow for changes in circuit parameters and drive pulses, core S_2 should finish switching before core C_2, and core C_2 should finish switching before core S_1.

Nonresistive Coupling Loop

The circuit shown in Fig. 7 is an example of a magnetic core shift register with a nonresistive coupling loop. This circuit was

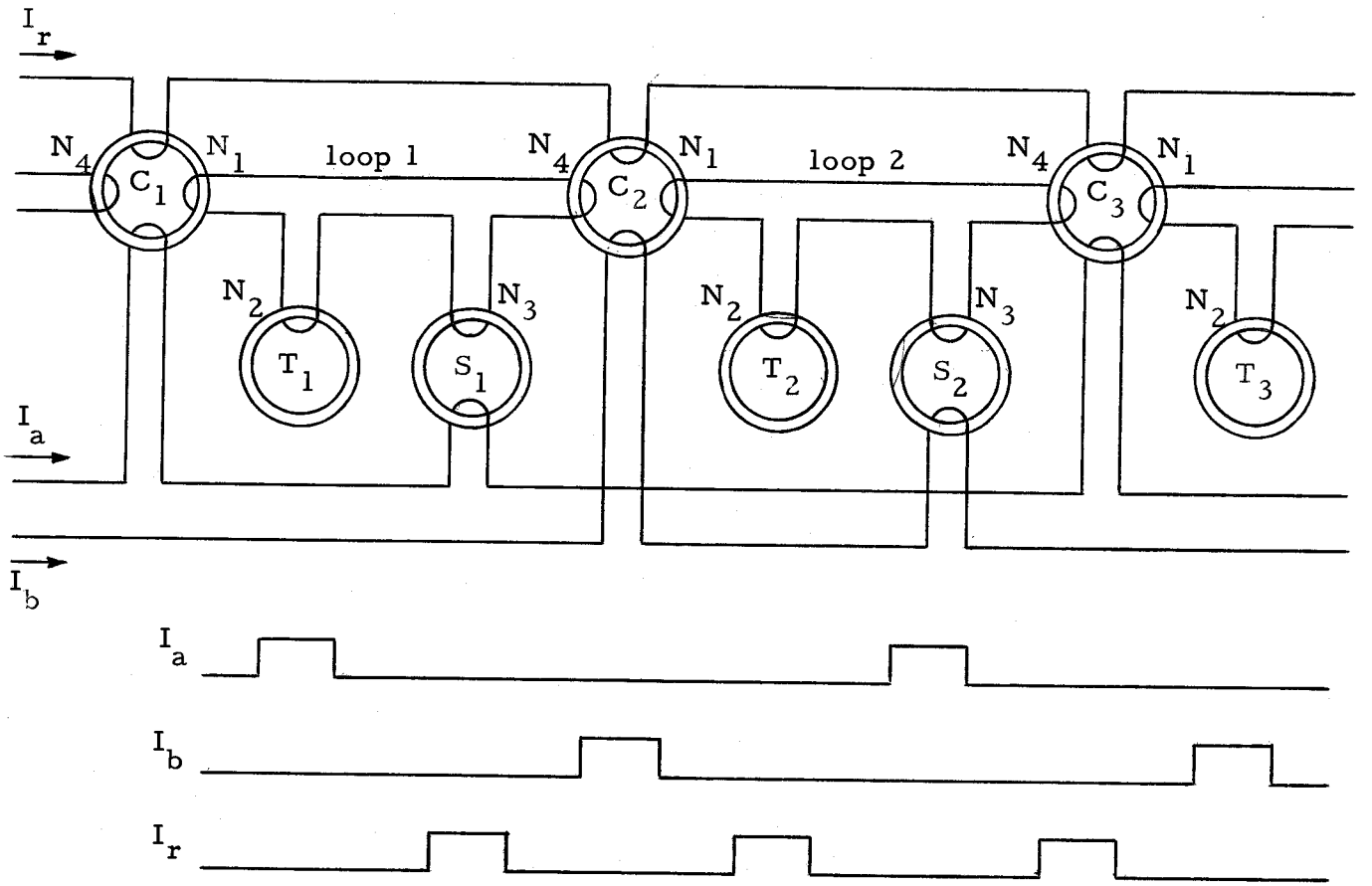

Fig. 7. Magnetic-core shift register with nonresistive coupling loop.

proposed by Yochelson (11). Inclusion of a resistance in the coupling loop of the circuit shown in Fig. 6 might be thought of as providing a means to dissipate excess energy delivered to the coupling loop by the switching of cores. In a nonresistive coupling loop the resistance is reduced to as near zero as possible, and an additional core is used to dissipate excess energy delivered to the loop. For the sake of clarity, certain bias-current windings have been omitted from the circuit shown in Fig. 7. A bias current will produce an mmf which will be less than the threshold mmf of a core. Positive and negative bias currents will tend to switch flux in a core in the clockwise and counterclockwise directions respectively. As before, a ONE will be represented by a clockwise setting of flux and a ZERO by a counterclockwise setting.

It will be assumed that cores S_1 and T_1 initially are in the ONE state, and the remainder of the cores are in the ZERO state. When current pulse I_a occurs it will set core S_1 to the ZERO state, and a voltage will be induced in winding N_3 which will cause a current to flow in the counterclockwise direction in loop one. This current will tend to set cores C_1 and C_2 to the ONE state and core T_1 to the ZERO state. Switching of flux in core C_1 is prevented by current pulse I_a which holds that core in the ZERO state. A positive bias current is applied to core T_1 during the time of current pulse I_a. The coupling-loop current would have to produce an mmf of nearly twice the value

of the threshold mmf of core T_1 to set that core to the ZERO state. A positive bias current is also applied to core C_2. To switch that core, the coupling-loop current must produce an mmf which is the difference between the mmf produced by the positive bias current and the positive threshold mmf of the core. Therefore, core C_2 will be set to the ONE state; and the coupling-loop current will be limited to a value below that required to switch core T_1. The switching of core C_2 will cause a clockwise current in loop two which will set core T_2 to the ONE state. The current in the second coupling loop will tend to set cores S_2 and C_3 to the ZERO state; but because these cores are already in the ZERO state, no change will take place in them. Thus, the setting of core S_1 to the ZERO state by current pulse I_a has caused cores C_2 and T_2 to be set to the ONE state. Current pulse I_r will now set core C_2 to the ZERO state causing counterclockwise currents in loops one and two. The coupling-loop currents will have no effect on cores C_1 and C_3 because these cores are held in the ZERO state by current pulse I_r. Because cores C_1 and C_3 do not switch at this time, information is not transferred outside of loops one and two; and back-transfer is prevented. At the same time that current pulse I_r is applied to core C_2, a positive bias current is applied to core T_2; and a negative bias current is applied to core T_1. The current in loop one which results from the switching of core C_2 will tend to switch core T_1 to the ZERO state and core S_1 to the ONE

state. But, because of the bias current applied to core T_1, this core will be switched to the ZERO state and core S_1 will remain in the ZERO state. The current in loop two will tend to switch core T_2 to the ZERO state and core S_2 to the ONE state; but the bias on core T_2 will hold this core in the ONE state, and core S_2 will be switched to the ONE state. The ONE's originally contained in cores S_1 and T_1 have been transferred to cores S_2 and T_2. Subsequent application of current pulses I_b and I_r and the bias-current pulses will transfer the ONE's to cores S_3 and T_3.

Voltage equations can be written for coupling loops one and two in Fig. 7 during the times that current pulses I_a and I_r are applied. Because it is physically impossible to construct a coupling loop without losses, it will be assumed that losses in each coupling loop can be represented by a resistance R. The voltage equations for loops one and two during the time of current pulse I_a are

$$N_3 \frac{d\phi_{s1}}{dt} = Ri_1 + N_4 \frac{d\phi_{c2}}{dt} \tag{11}$$

$$N_1 \frac{d\phi_{c2}}{dt} = Ri_2 + N_2 \frac{d\phi_{t2}}{dt} \tag{12}$$

During the time of current pulse I_r, the voltage equations for loops one and two are

$$N_4 \frac{d\phi_{c2}}{dt} = Ri_1 + N_2 \frac{d\phi_{t1}}{dt} \tag{13}$$

$$N_1 \frac{d\phi_{c2}}{dt} = Ri_2 + N_3 \frac{d\phi_{s2}}{dt} \tag{14}$$

The flux in cores S_1, S_2, T_1, T_2 and C_2 is represented by ϕ_{s1}, ϕ_{s2}, ϕ_{t1}, ϕ_{t2}, and ϕ_{c2} respectively; N_1, N_2, N_3, and N_4 represent the number of turns on the windings shown in Fig. 7; and i_1 and i_2 are the currents in coupling loops one and two respectively. If it is assumed that information is maintained at the maximum ONE level, then the flux change in all the cores involved will be $2\phi_r$. Under this assumption equations (11) through (14) can be integrated and rearranged as follows:

$$2\phi_r(N_3-N_4) = R\int i_1 dt \tag{15}$$

$$2\phi_r(N_1-N_2) = R\int i_2 dt \tag{16}$$

$$2\phi_r(N_4-N_2) = R\int i_1 dt \tag{17}$$

$$2\phi_r(N_1-N_3) = R\int i_2 dt \tag{18}$$

The last four equations indicate that the number of turns on the coupling loop windings must satisfy the following inequality.

$$N_1 > N_3 > N_4 > N_2 \tag{19}$$

FLUX TRANSFER CHARACTERISTIC

The coupling-loop voltage equations written for the circuits shown in Fig. 6 and 7 each involve two terms pertaining to cores and one resistance term. The coupling-loop equation of the circuit shown in Fig. 8 will have the same form as the equations for the circuits shown in Fig. 6 and 7. The coupling-loop voltage equation during the time of current pulse I_a is

$$N_1 \frac{d\phi_1}{dt} = Ri + N_2 \frac{d\phi_2}{dt} \qquad (20)$$

where ϕ_1 and ϕ_2 represent the flux in cores C_1 and C_2 respectively. Equation (20) can be integrated and solved for ϕ_2.

$$\phi_2 = \frac{N_1}{N_2}\phi_1 - \frac{R}{N_2}\int i\,dt \qquad (21)$$

Equation (21) represents the flux transfer characteristic of the coupling loop shown in Fig. 8.

When the flux in core C_1 is switched by current pulse I_a (Fig. 8), the voltage waveform induced in winding N_1 will be similar to the waveforms shown in Fig. 9. The largest waveform shown in Fig. 9 (acf) will occur when the flux in core C_1 is switched from $+\phi_r$ to $-\phi_r$ (Fig. 1). If the initial flux level in the core is less than $+\phi_r$, switching the flux to $-\phi_r$ will result in a waveform similar to ace. A still lower initial flux level might result in waveform abd.

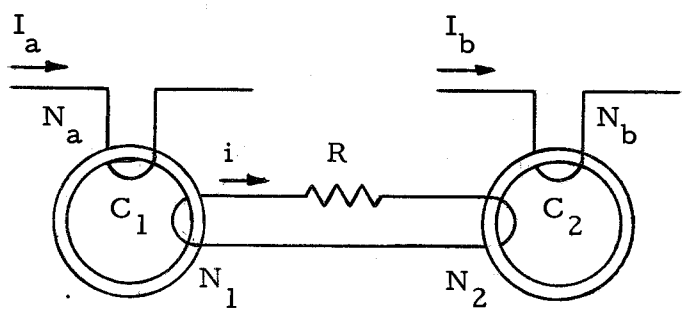

Fig. 8. Basic transfer circuit.

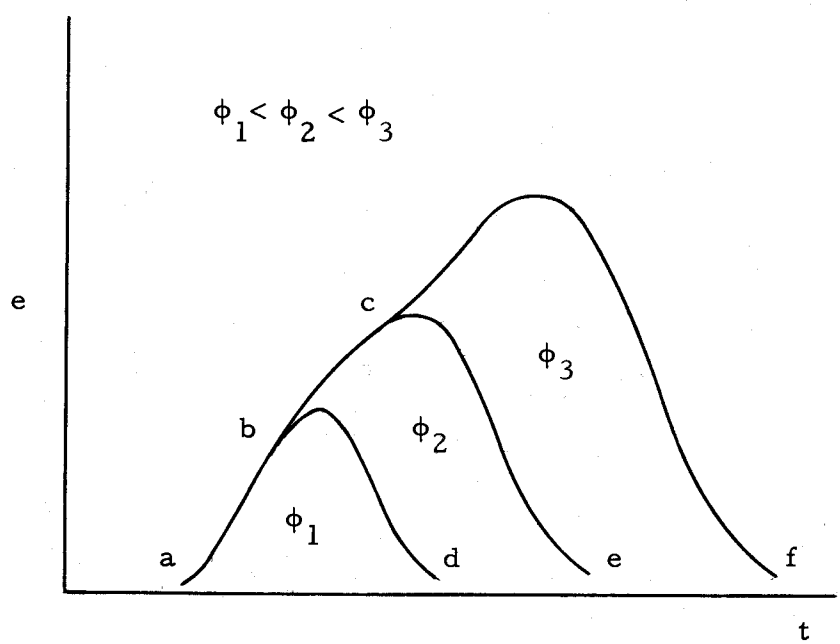

Fig. 9. Voltage waveforms resulting from different amounts of flux change in a magnetic core.

Because the amplitude of the voltage waveform induced in winding N_1 shown in Fig. 8 depends on the flux level in core C_1, the current which flows in the coupling loop will also depend on the flux level. When the flux in core C_1 is switched from a certain level to $-\phi_r$, the resulting coupling-loop current will produce an mmf which is equal to the threshold mmf of core C_2. There will be no inelastic flux switched in core C_2 if the flux level in core C_1 is less than this critical level. If the amount of flux switched in core C_1 is larger than this critical level, inelastic flux will be switched in core C_2; and the amount of flux switched will increase as the amount of flux in core C_1 is increased. At some high level of flux in core C_1, the amount of flux switched in core C_2 will be $2\phi_r$. That is, the flux in core C_2 will be switched from $-\phi_r$ to $+\phi_r$. Further increase of the amount of flux switched in core C_1 will not cause an increase of the flux level in core C_2. A plot of ϕ_2, the amount of flux switched in core C_2, versus ϕ_1, the amount of flux switched in core C_1, might be similar to the flux transfer characteristic abcd shown in Fig. 10. If ϕ_1 is less than ϕ_b, the value at point b in Fig. 10, only elastic flux will be switched in core C_2. Values of ϕ_1 greater than ϕ_c will not cause the amount of flux in core C_2 to exceed ϕ_{2s}, because this is the maximum amount of flux that can be switched in that core.

Because the quantities ϕ_{2r} and ϕ_{2s} shown in Fig. 10 primarily depend on core characteristics, the minimum and maximum values of

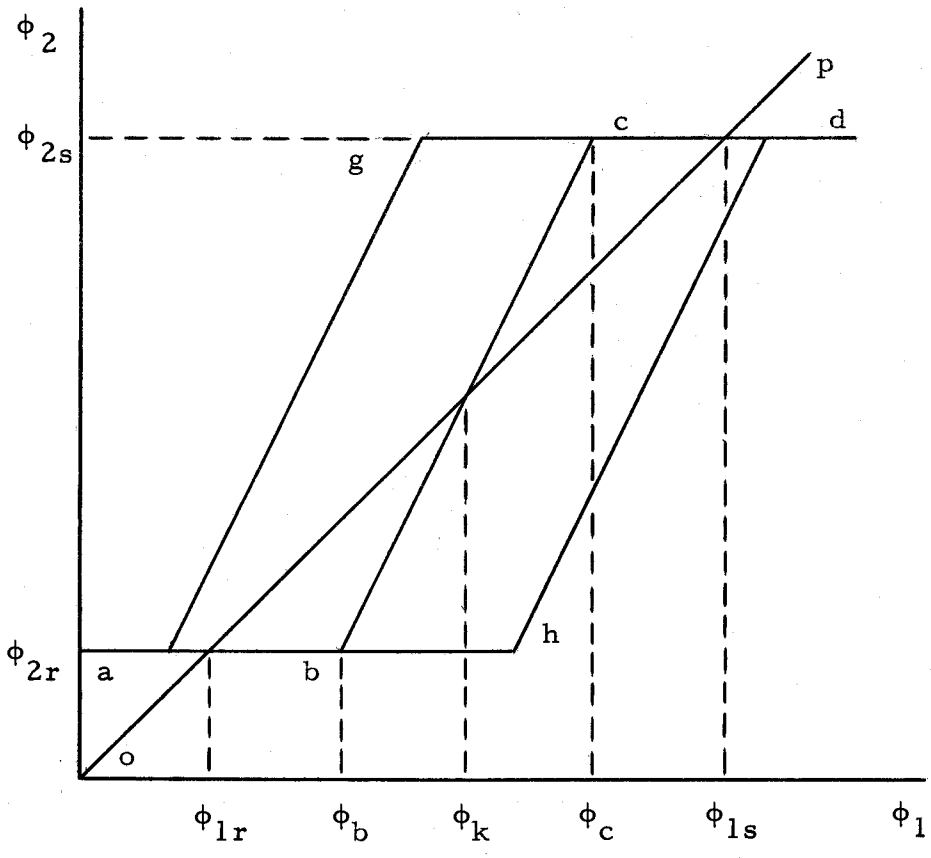

Fig. 10. Transfer characteristics and unity-gain line op.

ϕ_2 are fixed for a given type of core. The position of the flux transfer characteristic from the ϕ_2 axis is a function of the coupling-loop parameters. If the number of turns on windings N_1 and N_2 and the resistance have the proper values, the flux transfer characteristic of the circuit shown in Fig. 8 will be similar to characteristic abcd shown in Fig. 10. A reduction of the value of the resistance will cause the coupling-loop current to increase for a given amount of flux switched in core C_1. Consequently, the amount of flux change ϕ_1 in core C_1 at which inelastic flux will begin to be switched in core C_2 will be reduced. Because the coupling-loop current increases as the resistance decreases, the term $(R/N_2)\int idt$ in equation (21) will remain roughly constant as the resistance is varied; and the shape of the central portion of the transfer characteristic (from point b to point c) will be somewhat insensitive to variation of the resistance. Thus, a reduction of the resistance will move the flux transfer characteristic to the left (to position agd for example); and an increase of the resistance will move the characteristic to the right. Variation of the number of turns on windings N_1 and N_2 will affect both the position and shape of the flux transfer characteristic. Because of economic reasons the number of turns on coupling loop windings is normally made as small as possible; and, therefore, the effects of winding variations will not be considered.

The capability of a magnetic-core circuit to maintain an

information signal represented by a flux change at its proper level depends on the position of the transfer characteristic with respect to the line op shown in Fig. 10. If flux gain is defined as the ratio of ϕ_2 to ϕ_1, gain in the region above line op is greater than one; gain in the region below line op is less than one; and on line op the flux gain is equal to one. A circuit which has a transfer characteristic positioned as characteristic abcd shown in Fig. 10 will amplify a flux change which is between ϕ_k and ϕ_{ls} or less than ϕ_{lr}, and a flux change between ϕ_{lr} and ϕ_k or greater than ϕ_{ls} will be attenuated. A flux change in a shift register composed of transfer circuits which have the transfer characteristic abcd will be amplified or attenuated as it is transmitted from stage to stage. Depending on its original level, the flux change will be stabilized at either ϕ_{ls} of ϕ_{lr}. If the transfer circuits of a shift register have characteristic agd, flux changes in the register will be stabilized only at ϕ_{ls}. Circuits with transfer characteristic ahd will cause flux changes to stabilize at ϕ_{lr}.

COUPLING LOOP WITH SINGLE-TURN WINDINGS

It seems judicious to assume that the cost of placing a winding on a toroidal core is more or less directly related to the number of turns on the winding. Consequently, it is economically important to use the least possible number of turns. Equation (21) can be solved for flux gain.

$$\frac{\phi_2}{\phi_1} = \frac{N_1}{N_2} - \frac{R}{N_2\phi_1}\int i dt \qquad (22)$$

Because of the required position of the transfer characteristic (characteristic abcd shown in Fig. 10), the gain of a transfer circuit must be greater than one over some range of ϕ_1 in equation (22). Equation (22) indicates that the least number of turns which will produce a gain greater than one is two and one turns on windings N_1 and N_2 respectively. The windings N_a and N_b shown in Fig. 8 can be reduced to one turn each, and the required mmf can be obtained by increasing the amplitudes of current pulses I_a and I_b. Thus, winding N_1 is the only winding in the transfer circuit shown in Fig. 8 which must have more than one turn.

A description of a transfer circuit using toroidal cores and having only single-turn windings in the coupling loop has not been found in the literature. However, a circuit using multiaperture cores and having a coupling loop with single-turn windings was described by Crane

and Van De Riet (4, p. 211-212). This circuit utilized the characteristic of multiaperture cores that enables the transfer of information from a core without destruction of the information in the core. When a ONE is transferred from core C_1 to core C_2 in the circuit shown in Fig. 8, the ONE in core C_1 can be thought of as being destroyed because core C_1 is set to the ZERO state. In the multiaperture circuit described by Crane and Van De Riet, a ONE is transferred to one of a pair of multiaperture cores; and the ONE is then nondestructively transferred to the second core. Information is transferred from the two cores by simultaneously applying a current pulse to them. Two single-turn windings, one on each of the cores, are connected in series; and these are connected to a single-turn winding on a third core. The arrangement of the single-turn windings in series is equivalent to a two-turn winding on a single core. This multiaperture-core circuit suggested a toroidal-core circuit having only single-turn windings in its coupling loop.

The basic component in the circuit to be described is two toroidal cores connected by a zero-resistance coupling loop as shown in Fig. 12a. The curve shown in Fig. 11 is derived from the curve shown in Fig. 3 by multiplying the ordinate of Fig. 3 by $2\phi_r$, the flux change which occurs when a core is switched from $-\phi_r$ to $+\phi_r$; and the ordinate is thereby converted to average time rate of change of flux or average voltage per turn. Equation (23), which is written

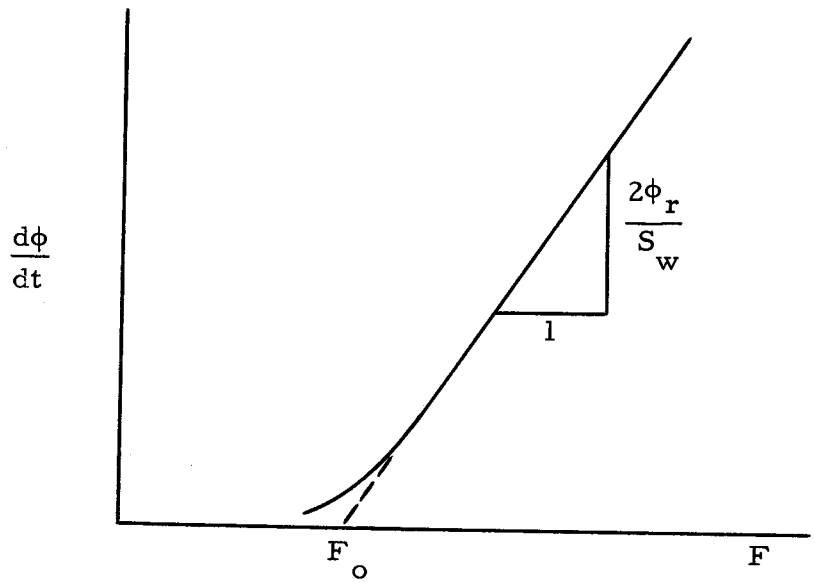

Fig. 11. Relationship between average voltage per turn and mmf derived from the switching characteristic of a core.

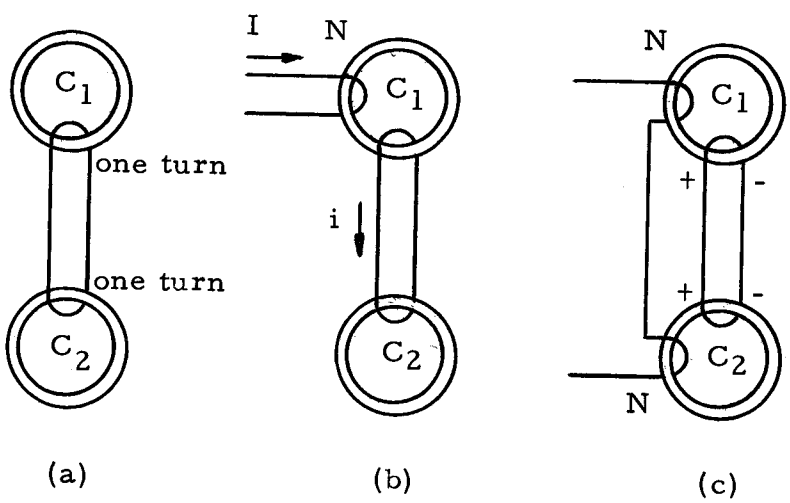

Fig. 12. Compound core made of two toroidal cores connected by a zero-resistance coupling loop.

for the linear portion of the curve shown in Fig. 11, relates the average time rate of change of flux in a core to the mmf (F) applied to the core.

$$\frac{d\phi}{dt} = \frac{2\phi_r}{S_w}(F-F_o) \tag{23}$$

Equation (23) can be written for cores C_1 and C_2 shown in Fig. 12b.

$$\frac{d\phi_1}{dt} = \frac{2\phi_r}{S_w}(F_1-F_o) \tag{24}$$

$$\frac{d\phi_2}{dt} = \frac{2\phi_r}{S_w}(F_2-F_o) \tag{25}$$

F_1 and F_2 are the mmf's applied to cores C_1 and C_2 respectively, and ϕ_1 and ϕ_2 are the fluxes in the cores. The mmf's acting to switch cores C_1 and C_2 are

$$F_1 = NI - i \tag{26}$$

$$F_2 = i \tag{27}$$

Substituting equations (25), (26), and (27) into equation (24) and rearranging yields

$$\frac{d\phi_1}{dt} + \frac{d\phi_2}{dt} = \frac{2\phi_r}{S_w}(NI-2F_o) \tag{28}$$

If it is assumed that the resistance of the coupling loop between cores C_1 and C_2 is in fact zero and the same amount of flux is switched in each core, then $d\phi_1/dt$ equals $d\phi_2/dt$. Under this assumption

equation (28) can be solved for $d\phi_1/dt$.

$$\frac{d\phi_1}{dt} = \frac{2\phi_r}{2S_w}(NI-2F_o) \tag{29}$$

Comparison of equations (29) and (23) shows that the circuit of Fig. 12b when viewed at winding N looks like a core with a threshold mmf of $2F_o$, a switching coefficient of $2S_w$, and a possible flux change of $2\phi_r$.

A current I applied as shown to the circuit in Fig. 12c will switch cores C_1 and C_2. If the two cores are identical and equal amounts of flux are switched in them, equal voltages with the polarities shown in Fig. 12c will be induced in the coupling loop. No current will flow in the loop, and the two cores will appear to be uncoupled. Therefore, when this circuit is viewed at the terminals of the series windings it will look like a core with characteristics F_o, S_w, and $4\phi_r$.

Two circuits like that shown in Fig. 12a can be connected to form a transfer circuit as shown in Fig. 13. It will be assumed that the flux in cores C_3 and C_4 is fully set in the counterclockwise direction and that the flux in cores C_1 and C_2 is set in the clockwise direction and at the same level in these cores. Current pulse I_a will switch the flux in cores C_1 and C_2 in the counterclockwise direction, and voltages will be induced in the N_1 windings in the coupling loop. The resulting coupling-loop current will switch flux in core C_3 in the

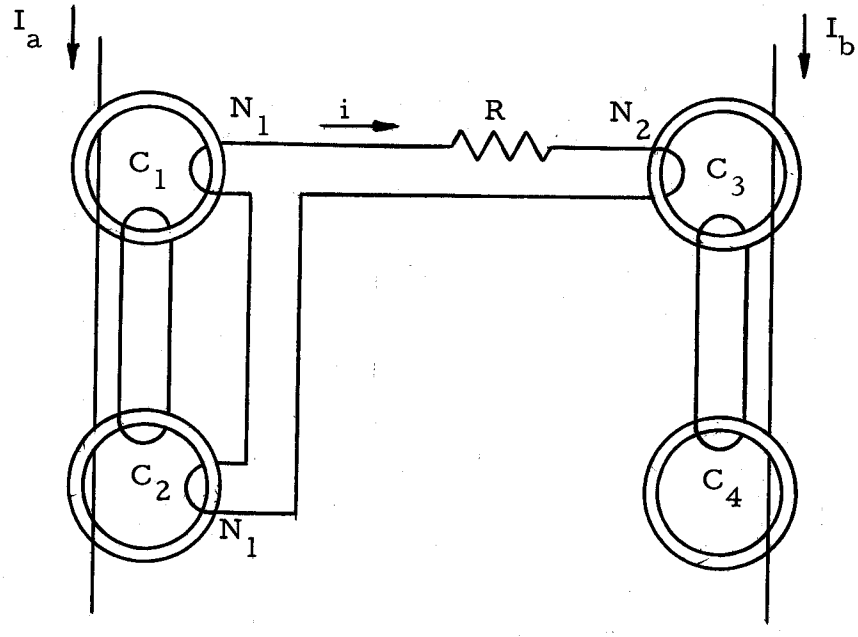

Fig. 13. Transfer circuit with a single-turn coupling loop.

clockwise direction, and the switching of core C_3 will cause flux in core C_4 to be switched in the clockwise direction. The coupling-loop voltage equation of the circuit in Fig. 13 during the time of current pulse I_a is

$$N_1\frac{d\phi_1}{dt} + N_1\frac{d\phi_2}{dt} = Ri + N_2\frac{d\phi_3}{dt} \tag{30}$$

If $d\phi_1/dt$ and $d\phi_2/dt$ are equal, equation (30) can be simplified; and integration will yield

$$2N_1\phi_1 = R\int i\,dt + N_2\phi_3 \tag{31}$$

This equation can be solved for flux gain.

$$\frac{\phi_3}{\phi_1} = 2\frac{N_1}{N_2} - \frac{R}{N_2\phi_1}\int i\,dt \tag{32}$$

Because of the term $2N_1/N_2$ in equation (32), it appears that the transfer circuit shown in Fig. 13 might be operable with one-turn windings in the coupling loop.

SINGLE AND COMPOUND CORE SWITCHING CHARACTERISTICS

The operation of the transfer circuit shown in Fig. 13 is based on the prediction that the compound core shown in Fig. 12a has different characteristics when viewed at different windings. The switching characteristics of the single core and the compound core shown in Fig. 14 were measured using the technique described in connection with the circuit and waveforms shown in Fig. 2. In both cases the measurements were made during the time of current pulse I_a. Current pulses I_a and I_b were furnished by the pulse source described in Appendix I. The circuits shown in Fig. 14 were used to obtain the switching characteristics shown in Fig. 15, and the threshold mmf F_o and switching coefficient S_w were obtained from the switching characteristics.

Table 1. Switching Constants of Single and Compound Cores.

	F_o(amp. turns)	S_w(amp. turn-μsec)
single core	0.33	0.45
compound core	0.70	0.80

The constants of the compound core given in Table 1 are approximately double the magnitude of the single-core constants. The variation from the predicted factor of two can probably be attributed to

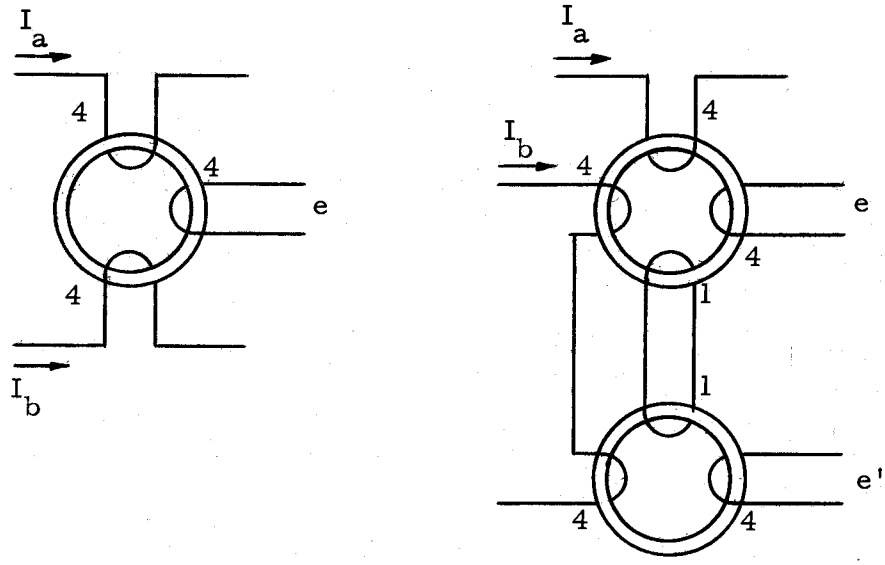

Fig. 14. Core circuits used to obtain switching characteristics.

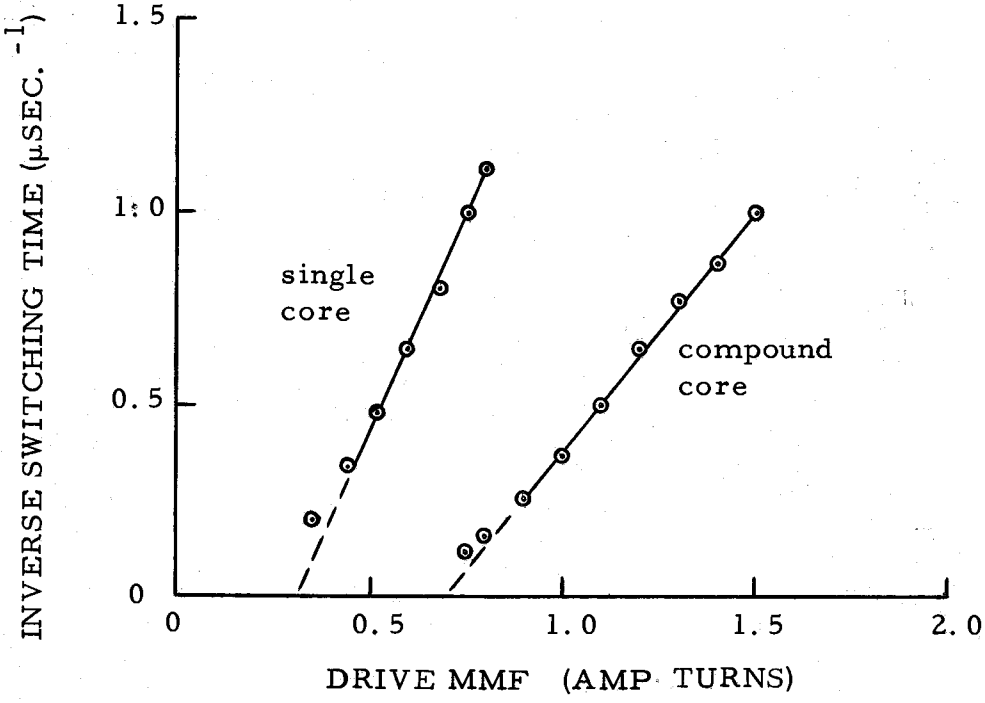

Fig. 15. Switching characteristics obtained from the core circuits shown in Fig. 14.

variations in dimensions and material properties of individual cores. The dimensions of the core (Radio Corporation of America type 222M1) are 0.080 inch outside diameter, 0.050 inch inside diameter and 0.025 inch height. The tolerance on the outside and inside diameters is $\pm$0.003 inch, and the tolerance on the height is $\pm$0.0025 inch. If the outside diameter of a core is at the upper limit and the inside diameter is at the lower limit, the radial thickness of the core will be 0.018 inch instead of the nominal 0.015 inch. Thus, a domain wall moving radially at constant velocity would require 20 percent more time to move from the inner wall to the outer wall of the core; and the switching time of the core would be increased. This would cause a decrease of the slope of the switching characteristic and an increase of the switching coefficient S_w of about 20 percent. Furthermore, the decrease of inside diameter would cause a decrease of the threshold mmf of the core of about six percent. The values of F_o and S_w obtained for the single and compound cores are within the variations that might be expected. Therefore, the results shown in Fig. 15 and Table 1 are a reasonable substantiation of the predicted characteristics of the compound core.

The voltage waveforms e and e' of the compound core shown in Fig. 14 were compared by superimposing them on an oscilloscope; no difference could be detected between the two waveforms. Therefore, the assumption that the rate of change of flux is the same for

the two cores is correct within the accuracy of the oscilloscope (five to 10 percent). The coupling loop of the compound core was made of approximately three quarters of an inch of number 22 AWG copper wire which was bent into a circle and soldered with a one eighthof an inch overlap.

TRANSFER CHARACTERISTICS AND GAIN MEASUREMENTS

To measure the gain and transfer characteristics of the transfer circuit shown in Fig. 13, the flux change in the cores must be measured. Because the voltage waveform induced in a winding on a core is proportional to the time derivative of the flux, the flux change can be measured by integrating the voltage waveform. An attempt was made to measure the flux change in a core by using an operational amplifier with the appropriate input and feedback components to integrate the voltage waveform induced in a winding. But because of the narrow width and low amplitude of the voltage waveform, this approach was unsatisfactory. The operational amplifier attenuated the voltage waveform to such an extent that it was necessary to reamplify the signal before displaying it on an oscilloscope. Because of the noise and instability added by the two amplifiers in cascade, the oscilloscope trace was useless.

A relative measurement of the flux change in a core can be made with a simple resistor-capacitor network. The application of a narrow pulse to the circuit shown in Fig. 16 will result in the indicated capacitor voltage waveform. The capacitor voltage will increase toward the pulse amplitude; and if the amplitude of the input pulse is constant, the voltage on the capacitor at time t_1 will depend on the width of the input pulse. An increase of the pulse width would

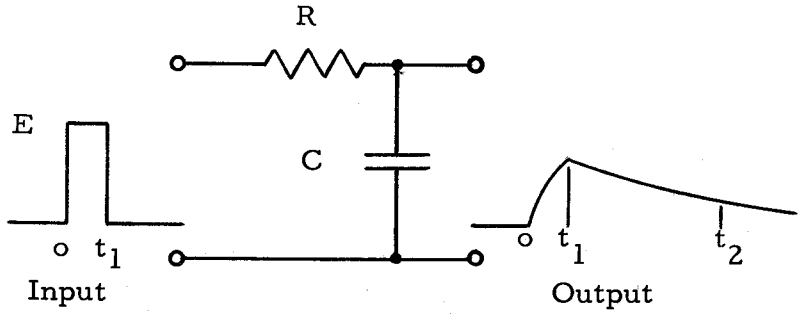

Fig. 16. Network configuration used to make relative measurements of flux change.

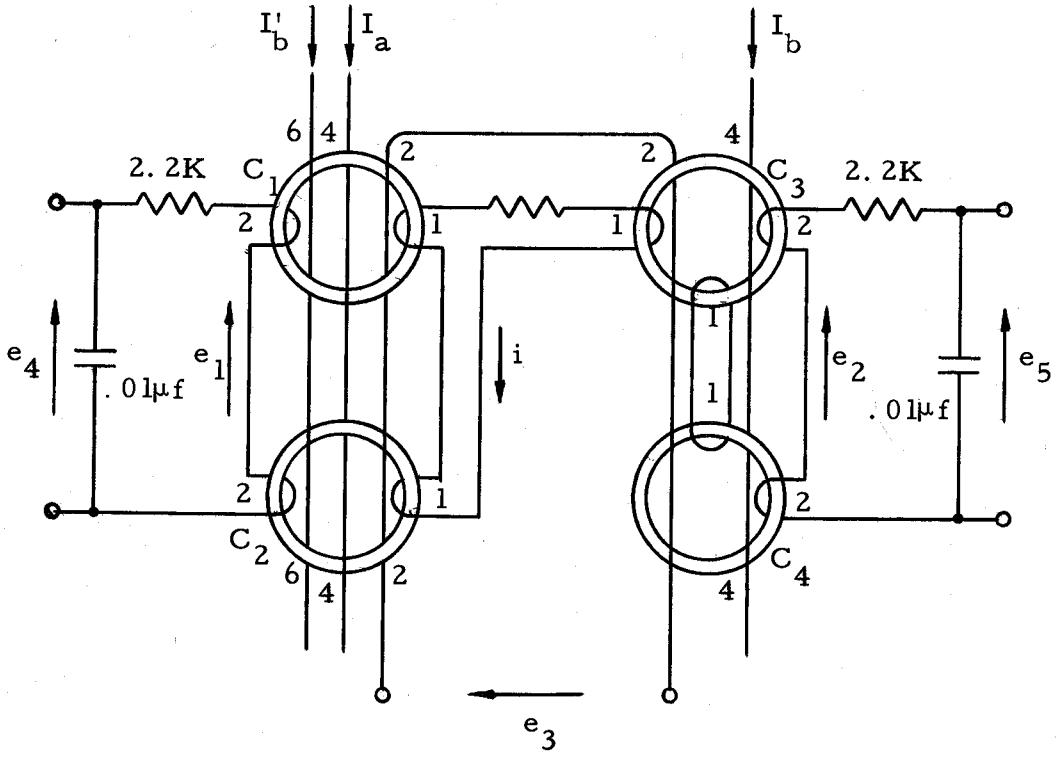

Fig. 17. Magnetic-core circuit on which transfer measurements were made.

allow a longer period of time for the capacitor to charge, and the capacitor voltage at time t_1 would increase. The voltage to which the capacitor will charge is also proportional to the pulse amplitude. Therefore, the voltage across the capacitor at time t_1 is proportional to the area under the input pulse. If the source of the input pulse has zero internal impedance, the voltage on the capacitor after time t_1 will depend only on the values of resistance and capacitance. At some time t_2 the capacitor voltage will have decayed to some percentage of the voltage at time t_1. Therefore, the capacitor voltage at time t_2 is proportional to the area of the input pulse. In Appendix 2 it is shown that if the ratio of the input pulse width to the product of resistance and capacitance is between 0.005 and 0.1, the error in the relative measurement of area of the input pulse will be within plus or minus three percent.

Measurements were made on the circuit shown in Fig. 17. The width of voltage waveforms e_1 and e_2 did not exceed two microseconds. The product of resistance and capacitance of measurement network was 22 microseconds. Therefore, measurement errors due to the network were less than three percent. Relative measurements of flux change were made on capacitor-voltage waveforms e_4 and e_5 at a point 15 microseconds after the beginning of current pulse I_a. The choice of 15 microseconds was a compromise. Prior to this time there was noise on waveforms e_4 and e_5; the noise was

apparently caused by the leading edge of current pulse I_a, disturbances on the d-c power supplies, and inductance in the measurement network. After this time the voltages across the capacitors were too low to be measured with any degree of accuracy.

In the transfer circuit shown in Fig. 17, the coupling loop between cores C_1 and C_2 was omitted because there was not enough space in the core apertures for the coupling loop and the other required windings. During the time that flux in cores C_1 and C_2 is being set in the counterclockwise direction by current pulse I_a, voltages induced in a coupling loop between these cores would have equal magnitudes and opposite directions around the loop; and cores C_1 and C_2 would appear to be uncoupled. Therefore, the omission of the coupling loop between cores C_1 and C_2 should not change the operation of the transfer circuit during the time of current pulse I_a. Relative measurements of flux change were made in the following manner. The flux in cores C_3 and C_4 was fully set in the counterclockwise direction by current pulse I_b, and a portion of the flux in cores C_1 and C_2 was simultaneously set in the clockwise direction by current pulse I'_b. Subsequently, the flux in cores C_1 and C_2 was set in the counterclockwise direction by current pulse I_a; and at this time, relative measurements were made of the flux changes in cores C_1 and C_2 and in cores C_3 and C_4. The amount of flux change in cores C_1 and C_2 was varied by changing the amplitude of current pulse I'_b.

The relative measurements of flux change were normalized; the base for this normalization was the measurement obtained when the flux in cores C_1 and C_2 changed from $+\phi_r$ to $-\phi_r$. The coupling loop between cores C_1 and C_2 and core C_3 was made of number 32 AWG copper wire. The value of resistance in the coupling loop was adjusted by varying the length of this wire.

The curves in Fig. 18, 19, and 20 depict the effects on the operation of the transfer circuit (Fig. 17) of varying coupling-loop resistance and drive current. The gain curves in Fig. 18 show that the magnitude of current pulse I_a affects the flux gain of the circuit but has little effect on the position of the curves, whereas both the gain and the position of the curves are affected by the value of the coupling-loop resistance.

The position of the transfer characteristics shown in Fig. 19 with respect to the unity-gain line is primarily a function of the value of resistance in the coupling loop. The voltage waveforms induced in the coupling-loop windings by flux changing in cores C_1 and C_2 will be similar to the waveforms shown in Fig. 9. The amount of flux change in cores C_1 and C_2 in the circuit in Fig. 17 must be greater than a certain level to cause inelastic-flux changes in cores C_3 and C_4. At levels of flux change in cores C_1 and C_2 below this critical level, the coupling-loop current depends on the resistance. If the resistance is increased, the amount of flux change in cores C_1 and

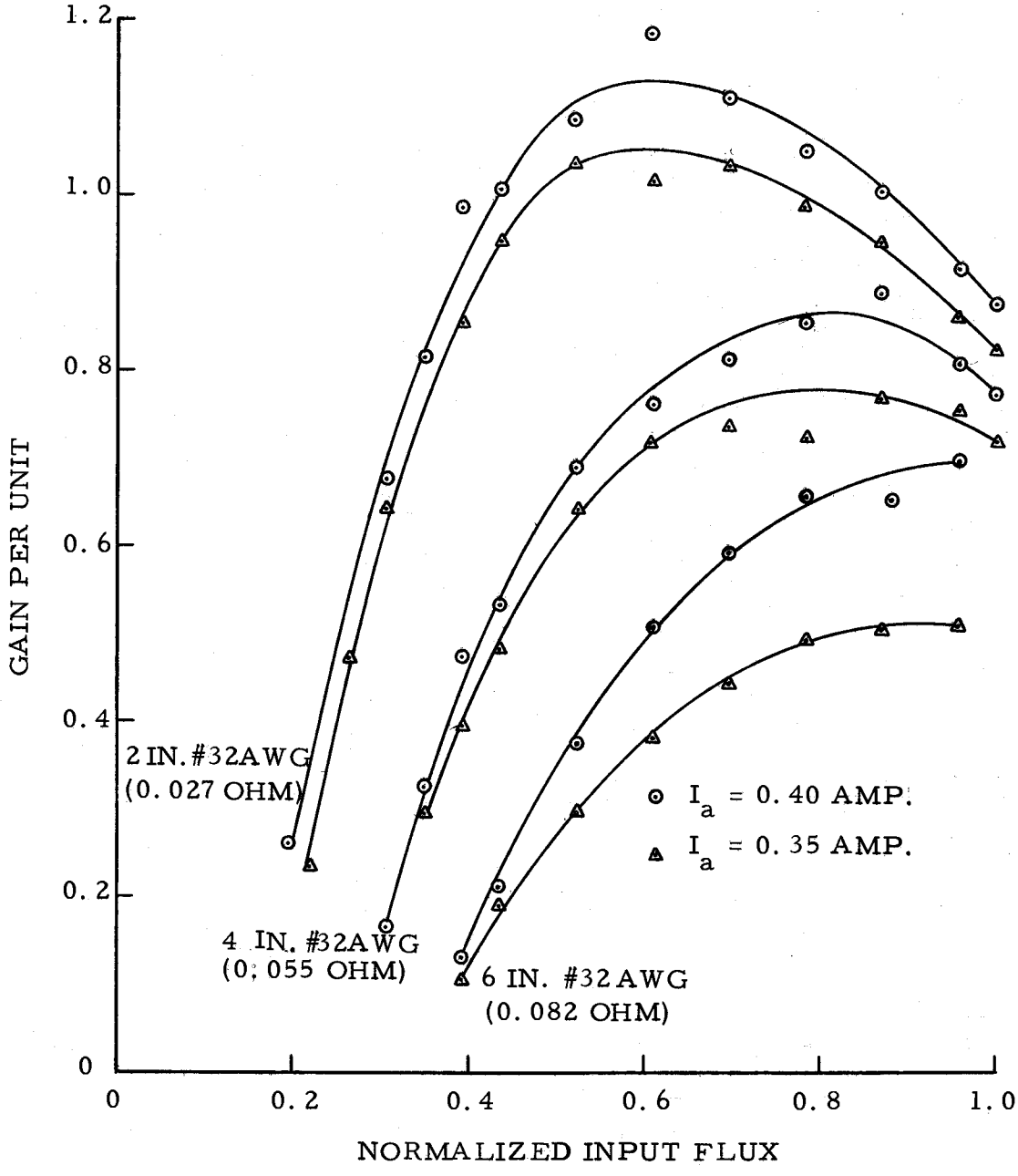

Fig. 18. Effect of coupling-loop resistance and drive current on gain characteristics of transfer circuit.

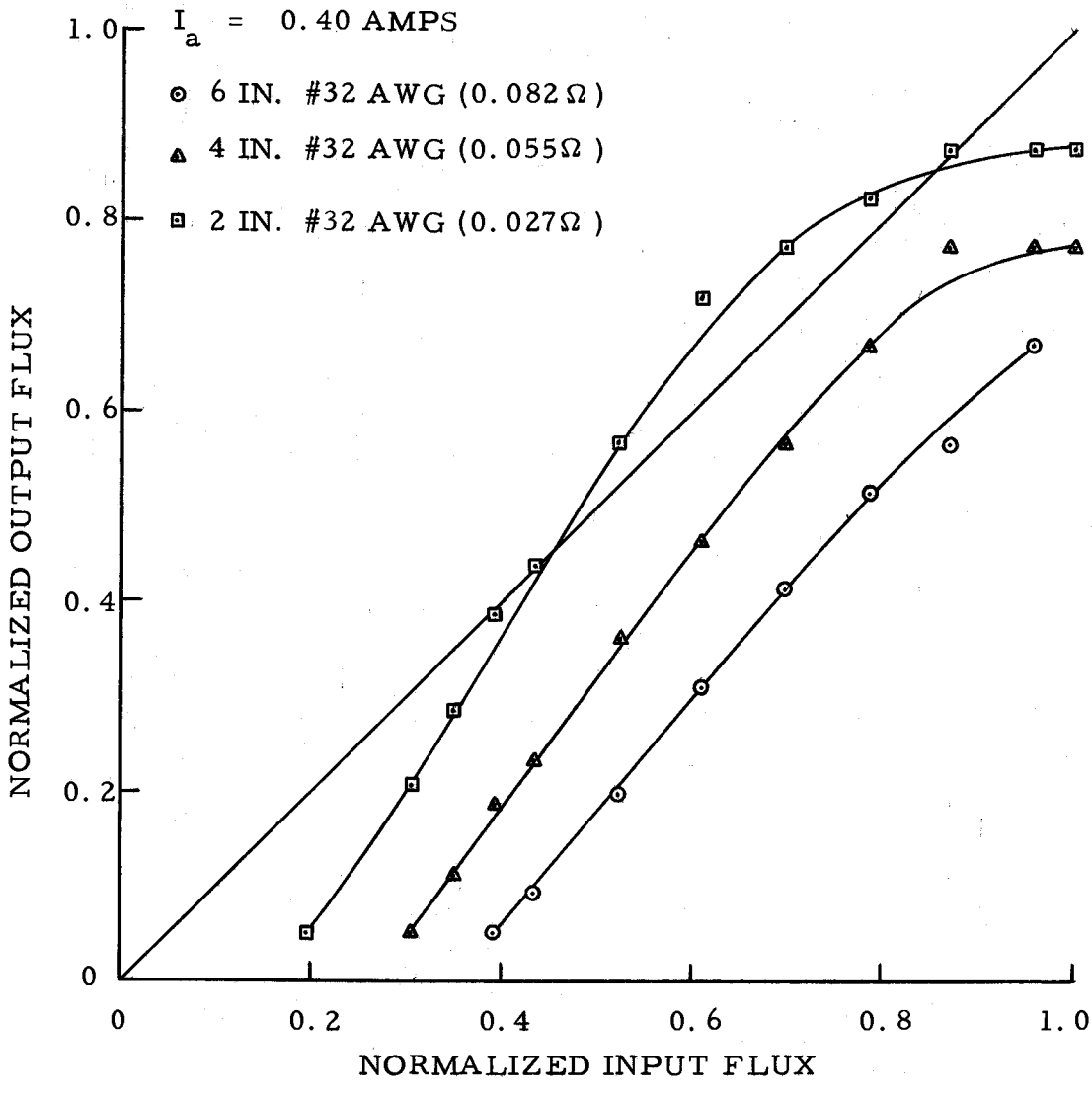

Fig. 19. Effect of coupling-loop resistance on transfer characteristics of transfer circuit.

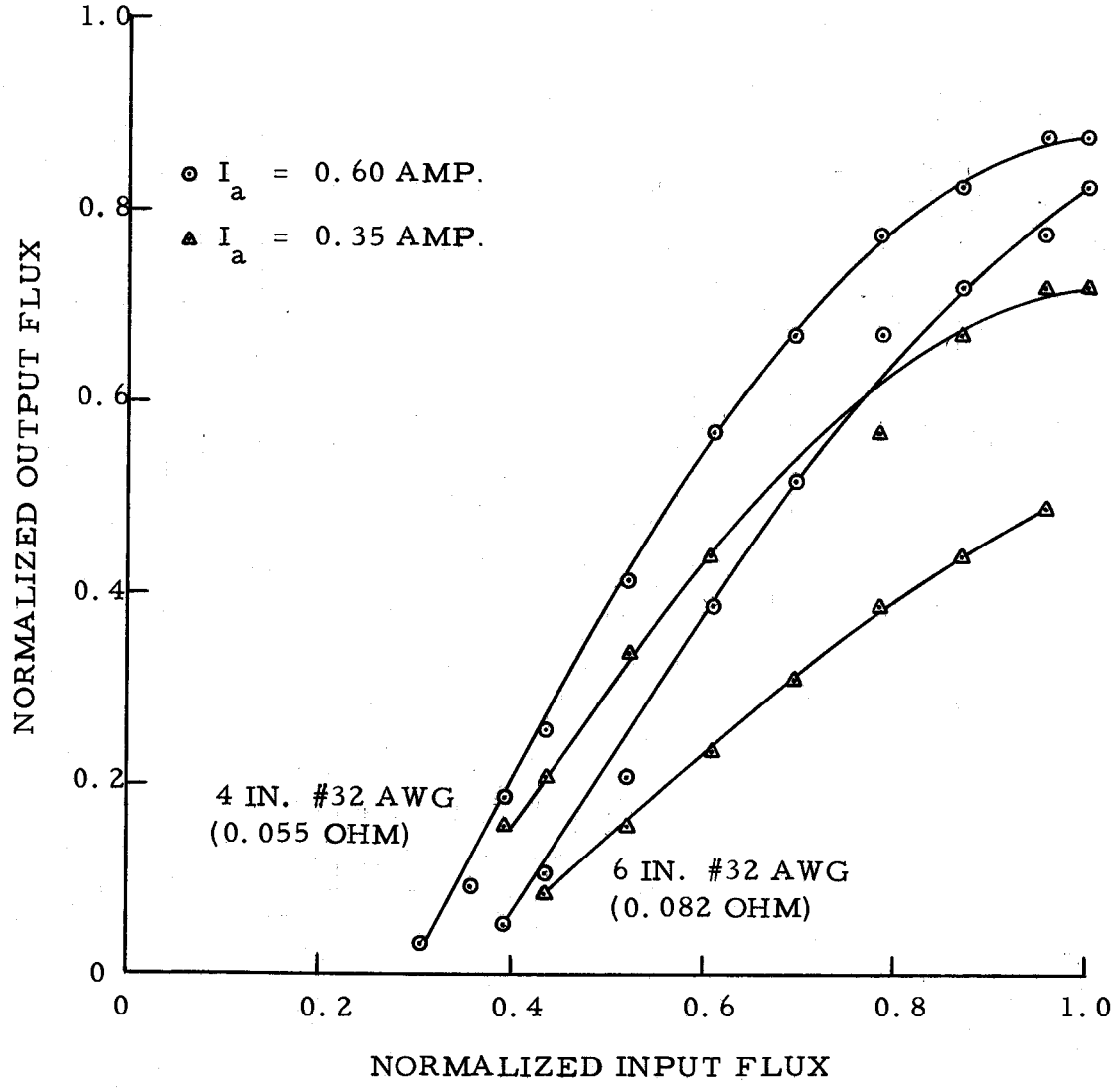

Fig. 20. Effect of drive current amplitude on flux transfer characteristics of transfer circuit.

C_2 must be increased to maintain a given magnitude of current in the coupling loop. Therefore, as shown by the curves in Fig. 19, the amount of flux change in cores C_1 and C_2 necessary to initiate inelastic-flux changes in cores C_3 and C_4 must be increased if the resistance is increased.

At intermediate levels of input flux, the shape of the transfer characteristics shown in Fig. 19 appears to be independent of the value of resistance. Equation (32) for flux gain can be solved for ϕ_3.

$$\phi_3 = \frac{2N_1}{N_2}\phi_1 - \frac{R}{N_2}\int i\,dt \qquad (33)$$

Two factors tend to cause the coupling-loop current i to remain constant as the resistance R is varied. First, an increase of the resistance will cause the coupling-loop current to decrease; the mmf acting to switch cores C_1 and C_2 (i.e., the difference between the mmf's produced by current pulse I_a and the coupling-loop current) will be increased, causing the amplitude of the voltage waveforms induced in the coupling loop to be increased; and the increased voltage will tend to increase the coupling-loop current. Therefore, the decrease of coupling-loop current caused by the increase of resistance will be partially offset. Secondly, because of the flux-mmf characteristic of the compound core composed of cores C_3 and C_4, changes of current in the coupling-loop winding on core C_3 will be restricted. The waveforms in Fig. 24d, 25d, 26d, and 27d show that during the

time the cores in the transfer circuit are switching the amplitude of the coupling-loop current i is not greatly affected by changes of resistance. For a given amount of flux change ϕ_1, the magnitude of the term $(R/N_2)\int idt$ in equation (33) will depend primarily on the value of the resistance; and the amount of flux change ϕ_3 also will be determined by the value of resistance. Therefore, the shape of the transfer characteristics will be somewhat independent of the value of the coupling-loop resistance.

As shown by the curves in Fig. 20, the slope of the flux transfer characteristic is influenced by the amplitude of the drive pulse. The two curves for each value of coupling-loop resistance converge as the input flux decreases. The amplitudes of current pulse I_a and coupling-loop current i shown in Fig. 25e are 0.6 and 1.4 amperes respectively. These currents produce an mmf of 1.0 ampere turn on cores C_1 and C_2, and the coupling loop current produces an mmf on core C_3 of 1.4 ampere turns. The curves in Fig. 21 show that these mmf's will cause a flux change of $2\phi_r$ in a single core and a compound core to occur in 0.6 and 1.1 microseconds respectively. If the amplitude of coupling-loop current is assumed to be directly proportional to the amplitude of drive current, then a current pulse of 0.35 ampere might cause switching times of a single and a compound core to be respectively 1.6 and 5.7 microseconds. In the transfer circuit shown in Fig. 17, the amount of flux change in the

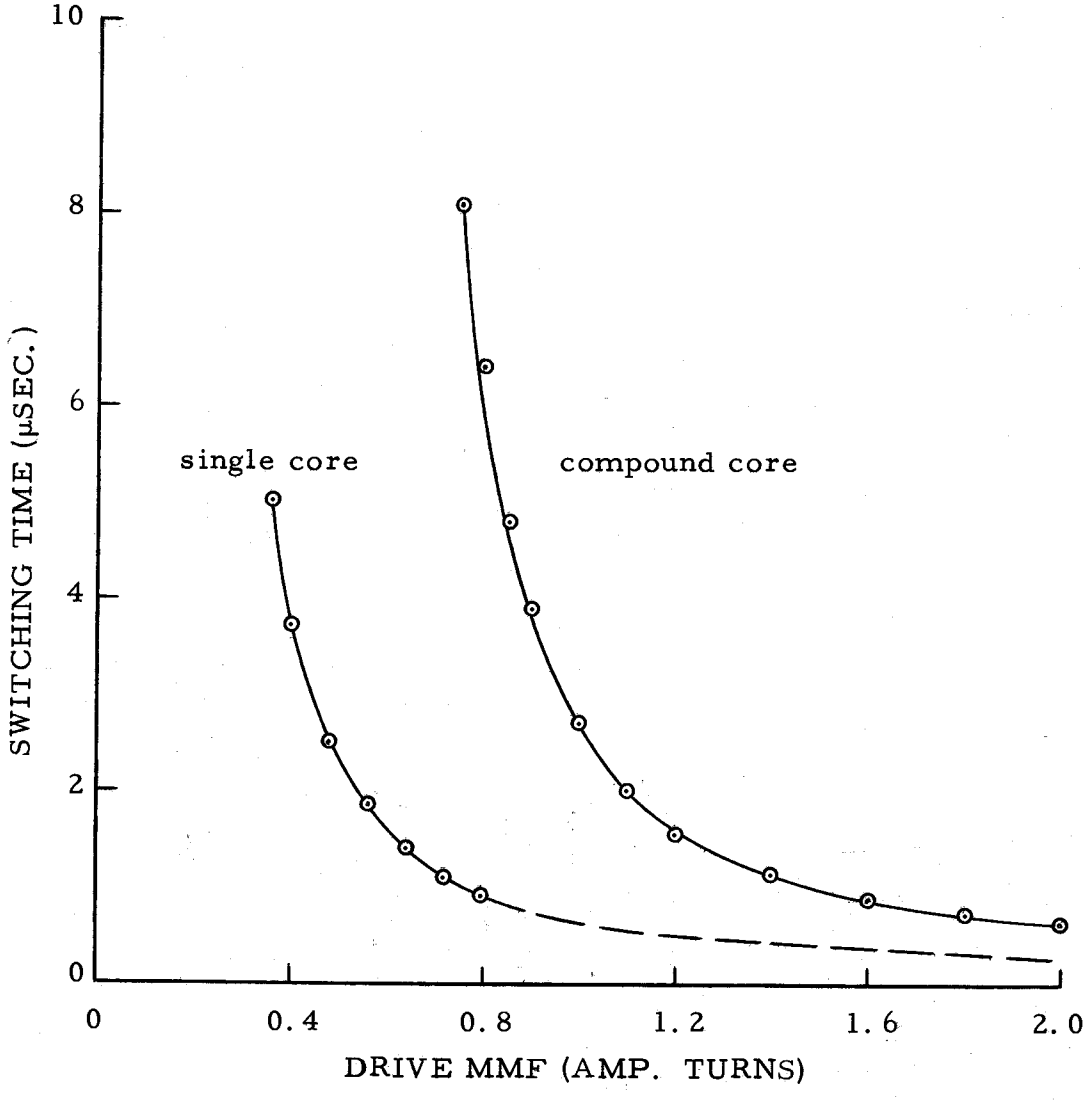

Fig. 21. Switching time versus applied mmf.

compound core (cores C_3 and C_4) will depend in part on the length of time that the mmf on core C_3 exceeds the threshold mmf; this time will be limited by the switching time of cores C_1 and C_2. As determined above, a current pulse of 0.6 ampere will restrict the time in which cores C_3 and C_4 can switch to 0.6 microseconds; but because of the mmf produced by the coupling loop current, these cores would require 1.1 microseconds for a full reversal of flux. Therefore, the flux change in cores C_3 and C_4 might be only 55 percent of the possible change. Similarly, a current pulse of 0.35 ampere might limit the amount of flux change in cores C_3 and C_4 to about 28 percent of its possible value. Because domain wall velocity, and consequently rate of change of flux, depends primarily on applied mmf, the amount of flux change in cores C_1 and C_2 should not affect the percentage of possible flux change that occurs in cores C_3 and C_4. Therefore, the ratio of flux changes caused in cores C_3 and C_4 by two different amplitudes of current pulse I_a should not be affected by the amount of flux change in cores C_1 and C_2. The previous approximations yield a ratio of flux changes in cores C_3 and C_4 of 0.51 for current pulses of 0.35 and 0.60 ampere and a coupling-loop resistance of 0.055 ohm. The two curves in Fig. 20 for a coupling-loop resistance of 0.055 ohm yield a ratio of output fluxes that varies between 0.77 and 0.85 over the range of normalized input flux from 0.5 to 1.0. The average ratio of output fluxes is 0.80. The

difference between the approximated ratio and the ratios obtained from the curves in Fig. 20 probably arises from the assumption that coupling loop current is proportional to drive current. Nevertheless, the approximations show that a reduction of drive current increases the time required for a flux change in cores C_3 and C_4 by a percentage which is greater than the percentage increase of the switching time of cores C_1 and C_2; and therefore, the amount of flux change in cores C_3 and C_4 is reduced.

The ratio of output fluxes obtained from the two curves in Fig. 20 for a coupling-loop resistance of 0.082 ohm varies from 0.72 to 0.60 over the range of normalized input flux from 0.5 to 1.0, and the average ratio is 0.63. The amplitude of coupling-loop current i for a resistance of 0.082 ohm and a drive pulse of 0.60 ampere shown in Fig. 26d is 1.3 ampere; this compares with the amplitude of coupling-loop current of 1.4 amperes shown in Fig. 25d for a resistance of 0.055 ohm. The lower value of coupling-loop current results in a decrease of the switching time of cores C_1 and C_2 and an increase of the time that would be required for a flux reversal in cores C_3 and C_4. The effects of reducing the amplitude of current pulse I_a will be similar to those described for the circuit with a coupling-loop resistance of 0.055 ohm. For the higher coupling-loop resistance, the decrease of mmf on the compound core occurs over a lower range of mmf; and the increase of time required for a

flux reversal in cores C_3 and C_4 will be greater than it was for the lower coupling-loop resistance. Higher resistance will cause the change of the switching time of cores C_1 and C_2 for the two values of drive current to be less. Therefore, as shown by the curves in Fig. 20, the ratio of output fluxes for two values of drive current and a given input flux will be less with a resistance of 0.082 ohm in the coupling loop than with a resistance of 0.055 ohm.

Although no mention has yet been made of coupling-loop inductance, the transfer characteristics in Fig. 22 show that it cannot be ignored. The labeling of the curves in Fig. 22 refers to the area enclosed by the coupling loop. Maximum-area loops were circular; area was minimized by collapsing a circular loop and twisting its sides together. The defining equation of inductance L is

$$L = N\frac{d\phi}{di} \tag{34}$$

For a coupling loop, ϕ represents the flux enclosed by the loop; and i represents the current in the coupling loop. N, which represents the number of turns enclosing the coupling-loop area, is one. The flux enclosed by a coupling loop of area A is given by

$$\phi = \int B \cdot dA \tag{35}$$

Because the flux density B at each point within the loop configuration is proportional to the current in the loop, the flux enclosed by the loop is proportional to the loop current. A reduction of loop area

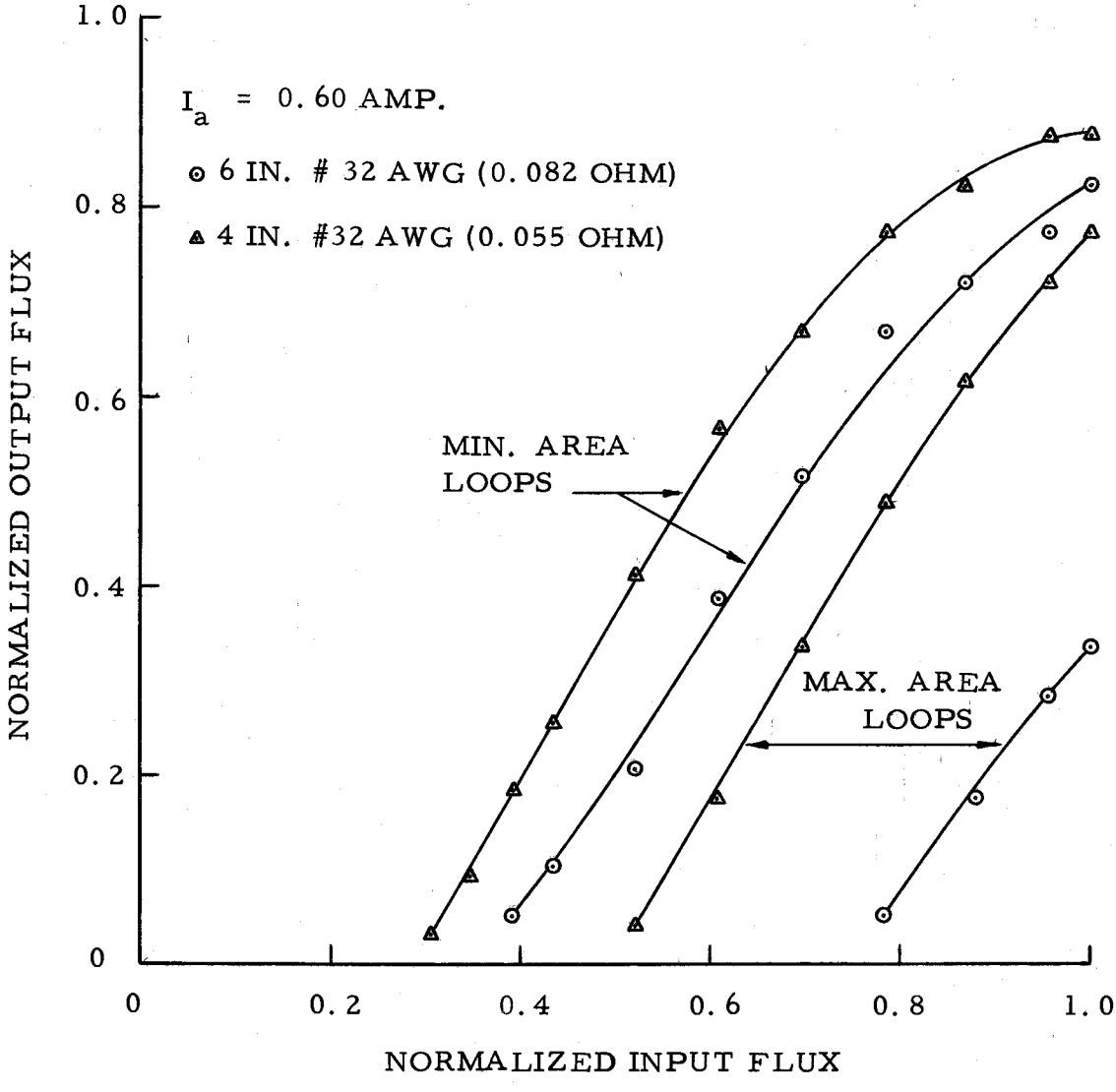

Fig. 22. Effect of coupling-loop inductance on transfer characteristics of transfer circuit.

will reduce the change of flux caused by a given change of current in the loop, and in accordance with equation (34) this will reduce the inductance of the loop.

The curves shown in Fig. 22 indicate that the coupling-loop inductance has an effect on the transfer characteristics which is similar to the effect of coupling-loop resistance. That is, the inductance appears to primarily affect the position of the characteristics. Inductance will limit the rate of increase of current in the coupling loop (see Fig. 26b and 26d). An increase of inductance will cause a decrease of the mmf on core C_3 and an increase of the mmf on cores C_1 and C_2; and consequently, the amount of flux change in cores C_3 and C_4 will be reduced for a given flux change in cores C_1 and C_2. Because of the reduction of mmf on core C_3, there must be an increase of flux change in cores C_1 and C_2 to initiate an inelastic-flux change in cores C_3 and C_4.

Because energy delivered to the coupling-loop inductance is temporarily stored but not dissipated, the decrease of the flux change in cores C_3 and C_4 caused by the inductance will be partially offset. This phenomenon is evident in waveforms e_1 and e_2 in Fig. 26a. The change of flux in cores C_3 and C_4, represented by the area of waveform e_2, continues after the change of flux in cores C_1 and C_2 has stopped. Because of the manner in which it was obtained (see Fig. 17), the area of waveform e_3 represents the difference between the

flux change in cores C_1 and C_2 and the flux change in core C_3; or the area of this waveform represents the coupling-loop loss. During the time that flux is changing in cores C_1 and C_2, waveform e_3 in Fig. 26b is positive, indicating that the coupling loop is absorbing energy. Waveform e_3 becomes negative as the flux in cores C_1 and C_2 stops changing. The coupling-loop inductance is then delivering energy which causes the flux to continue to change in cores C_3 and C_4.

The dependence of coupling-loop inductance on the circumference and area of the coupling loop is shown by the curves in Fig. 23. To avoid disturbing the characteristics of the coupling loop, the following method was employed to measure the inductance. A current was induced in the loop by placing it near a wire carrying a current pulse. The decay portion of the current waveform in the loop was observed on an oscilloscope using a current probe. This portion of the waveform is described by

$$i = I \epsilon^{-Rt/L} \qquad (36)$$

where i is the loop current, and R and L are respectively the resistance and inductance of the loop. Because of the form of equation (36), a plot of the waveform on semi-logarithmic graph paper was a straight line with a negative slope of R/L. The values of the slope and loop resistance enabled the calculation of loop inductance.

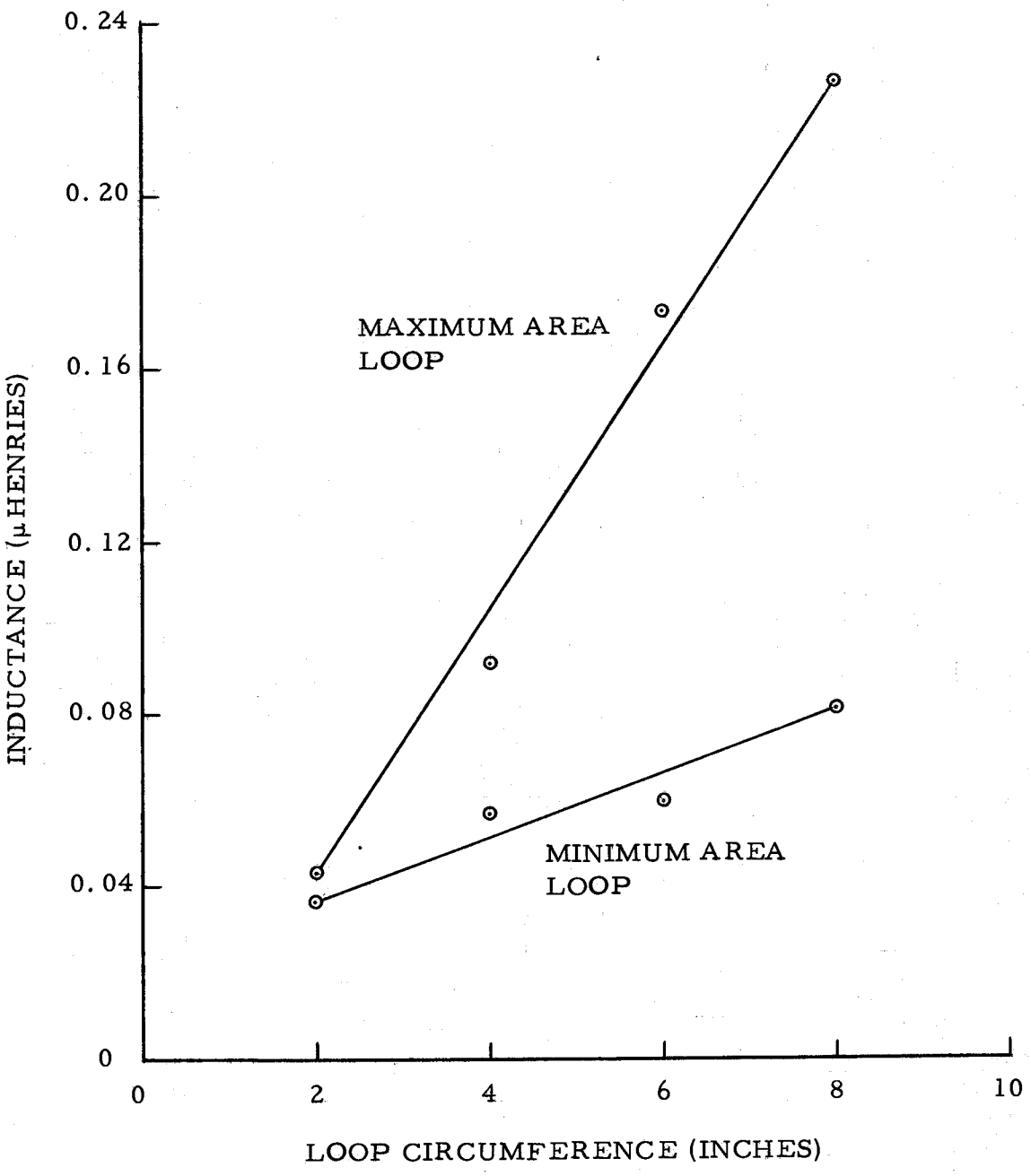

Fig. 23. Inductance versus circumference of coupling loop made of #32 AWG copper wire.

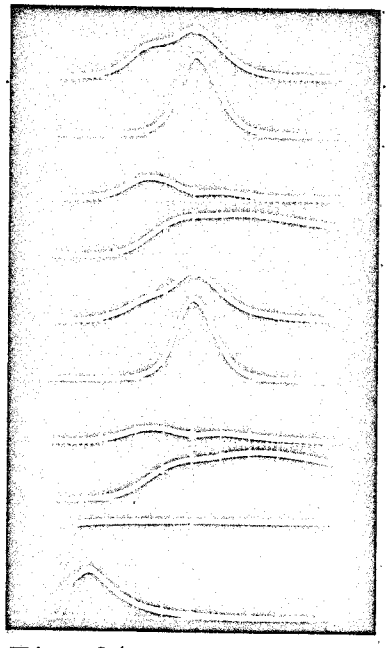

Fig. 24. Waveforms of circuit in Fig. 17 with 0.027 ohm coupling-loop resistance; (a) and (b) maximum coupling-loop area; (c), (d), and (e) minimum coupling-loop area.

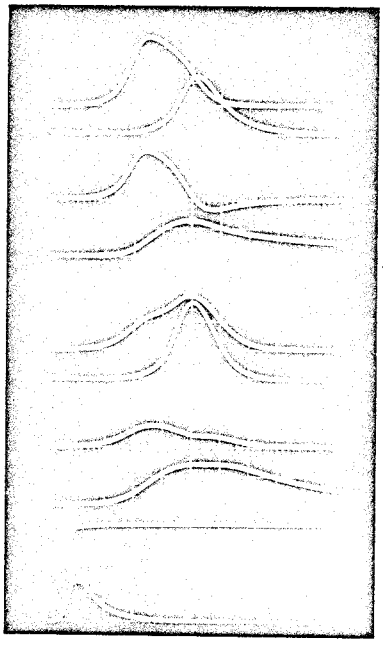

Fig. 25. Waveforms of circuit in Fig. 17 with 0.055 ohm coupling-loop resistance; (a) and (b) maximum coupling-loop area; (c), (d), and (e) minimum coupling-loop area.

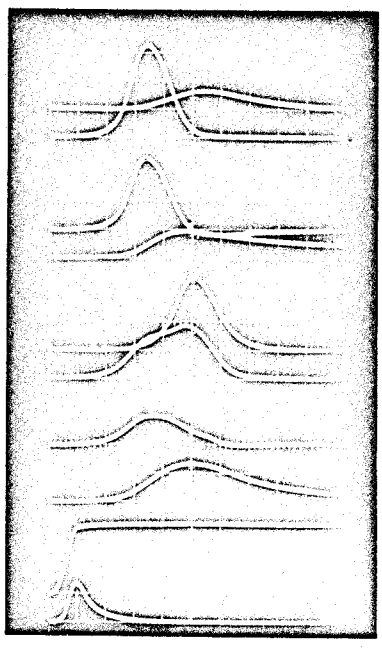

Fig. 26. Waveforms of circuit in Fig. 17 with 0.082 ohm coupling-loop resistance; (a) and (b) maximum coupling-loop area; (c), (d), and (e) minimum coupling loop area.

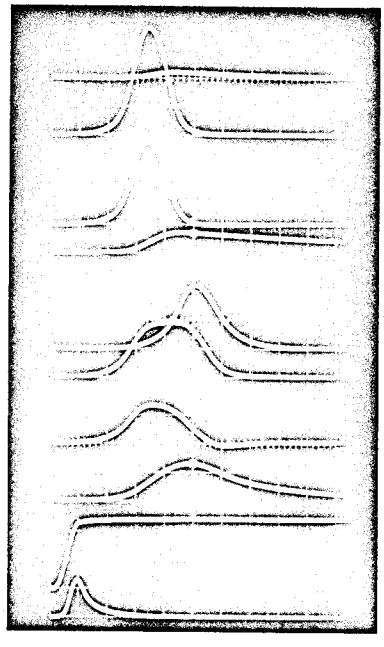

Fig. 27. Waveforms of circuit in Fig. 17 with 0.110 ohm coupling-loop resistance; (a) and (b) maximum coupling-loop area; (c), (d), and (e) minimum coupling-loop area.

SUMMARY AND CONCLUSIONS

Examination of the magnetic-core shift registers in Fig. 6 and 7 showed that the transfer process is basically the same in both circuits; and an analysis of the simple, two-core circuit shown in Fig. 8 yielded results which are applicable to the more complicated circuits. One result of the analysis was that the coupling-loop winding on a transmitting core must have a greater number of turns than the coupling-loop winding on a receiving core. This inequality of windings requires that the winding on the transmitting core must have more than one turn. From an economic viewpoint, the development of a circuit having only one-turn windings seems to be worthwhile. Analysis and experimental investigation of the circuit shown in Fig. 13 demonstrated the feasibility of a transfer circuit having only one-turn windings. It might be concluded from the test circuit shown in Fig. 22 that the drive windings require more than one turn. Multiple-turn windings were required only because the pulse source used could not provide sufficient mmf in a one-turn winding. Increasing the current capability of the pulse source should allow the use of one-turn windings.

Experimental investigation of the circuit in Fig. 17 showed that the amplitude of the drive pulse affects the shape of the transfer characteristic and that the position of the characteristic with respect to

the unity-gain line is determined by the value of coupling-loop resistance. The investigation also showed that the effects of coupling-loop inductance on the transfer characteristic are similar to those of coupling-loop resistance.

In the description of the shift register shown in Fig. 6, it was stated that the receiving core must finish switching before the transmitting core completes its switching. Because coupling-loop inductance delays the beginning of switching of a receiving core and allows a transmitting core to switch at a faster rate, it might be concluded that inductance is detrimental. The compound core switches at a slower rate when it is operating as a receiving core than when it is operating as a transmitting core. This is indicated by the different switching coefficients for the two modes of operation. The coupling-loop inductance can temporarily store energy. Therefore, the inductance might have an optimum value which would allow a receiving compound core to finish switching after the transmitting core had finished. This conjecture was prompted by the effects of coupling-loop inductance on the waveforms shown in Fig. 25 and 26.

BIBLIOGRAPHY

1. Bennion, D. R. MAD-resistance type magnetic shift registers. In: Proceedings of the Special Technical Conference on Nonlinear Magnetics and Magnetic Amplifiers, Philadelphia, 1960. New York, American Institute of Electrical Engineers, 1960. p. 96-112.

2. Bennion, D. R., H. D. Crane and D. C. Engelbart. A bibliographical sketch of all-magnetic logic schemes. Institute of Radio Engineers Transactions on Electronic Computers EC-10:203-206. 1961.

3. Betts, R. and G. Bishop. Ferrite toroid core circuit analysis. Institute of Radio Engineers Transactions on Electronic Computers EC-10:51-56. 1961.

4. Crane, H. D. and E. K. Van De Riet. Design of an all-magnetic computing system: part I - circuit design. Institute of Radio Engineers Transactions on Electronic Computers EC-10:207-220. 1961.

5. Gilli, L. and A. R. Meo. The behavior of rectangular hysteresis loop cores in every application. Proceedings of the Institute of Electrical and Electronics Engineers 51: 1578-1584. 1963.

6. Haynes, John L. Logic circuits using square-loop magnetic devices: a survey. Institute of Radio Engineers Transactions on Electronic Computers EC-10:191-203. 1961.

7. Karnaugh, M. Pulse switching circuits using magnetic cores. Proceedings of the Institute of Radio Engineers 43:570-584. 1955.

8. Menyuk, N. and J. B. Goodenough. Magnetic materials for digital-computer components. I. A theory of flux reversal in polycrystalline ferromagnetics. Journal of Applied Physics 26:8-18. 1955.

9. Russell, L. A. Diodeless magnetic core logical circuits. In: Institute of Radio Engineers National Convention Record, New York, 1957. pt. 4. New York, Institute of Radio Engineers, 1957. p. 106-114.

10. Wang, An and Way Dong Woo. Static magnetic storage and delay line. Journal of Applied Physics 21:49-54. 1950.

11. Yochelson, S. B. Diodeless core logic circuits. In: Institute of Radio Engineers WESCON Convention Record, Los Angeles, 1960. pt. 4. New York, Institute of Radio Engineers, 1960. p. 82-85.

APPENDIX I

A current pulse source for core circuits must deliver two or more noncoincident, electrically isolated pulses per cycle; and because an appropriate pulse source was not available, the circuits shown in Fig. 28 and 29 were designed. The circuit shown in Fig. 28 can be driven at its input by any convenient signal source (sine wave, square wave, etc.). Transistors Q_1 and Q_2 form a Schmitt circuit which produces a square voltage waveform at the collector of transistor Q_2. The primary of transformer T_1 and the two 1000 ohm collector resistors differentiate the collector waveform of transistor Q_2. Because of diodes D_1 and D_2 and the polarity of the secondary windings of the transformer, a positive pulse with a width of about five microseconds is obtained at each output. The pulse at output A occurs when transistor Q_2 turns on, and the pulse at output B occurs when transistor Q_2 turns off. Two circuits like that shown in Fig. 29 are required; one is driven by output A, and the other by output B of the trigger generator circuit shown in Fig. 28. Transistors Q_1 and Q_2 shown in Fig. 29 form a monostable multivibrator. A positive pulse applied to the input will cause this circuit to regenerate, and transistor Q_2 will be turned on for approximately 35 microseconds. Turn on of transistor Q_2 will cause transistor Q_3, which is normally off, to turn on; and when transistor Q_3 turns on, it will cause transistors

Q_4 and Q_5 to turn on. The separate voltage supplies of transistors Q_4 and Q_5 allow independent adjustment of the collector currents of these transistors. The main drive pulse was obtained from transistor Q_4, and the pulse obtained from transistor Q_5 was used to set variable levels of flux in cores as required for the transfer measurements. A block diagram of the complete pulse source and the timing of output pulses are shown in Fig. 30.

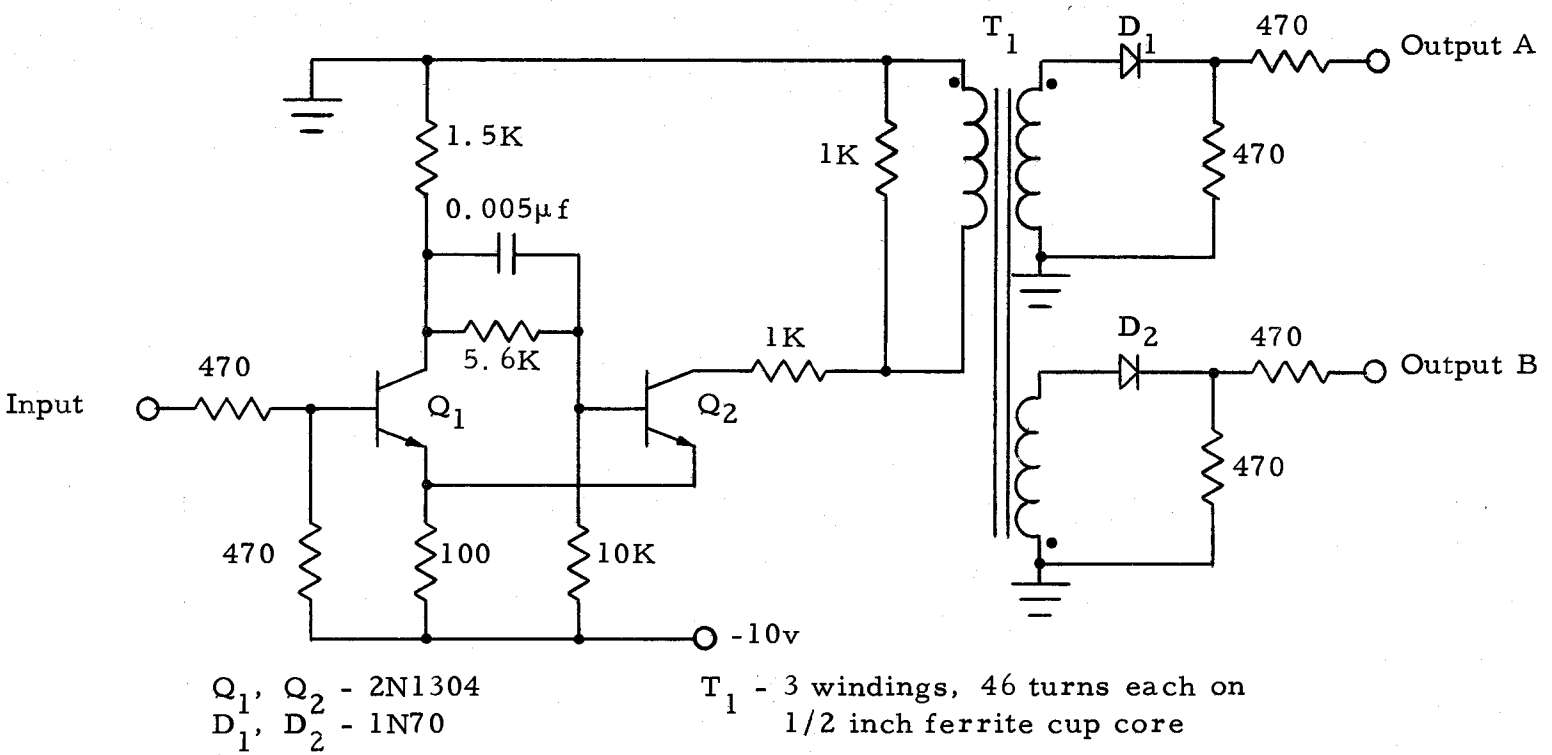

Fig. 28. Circuit diagram of trigger-pulse generator.

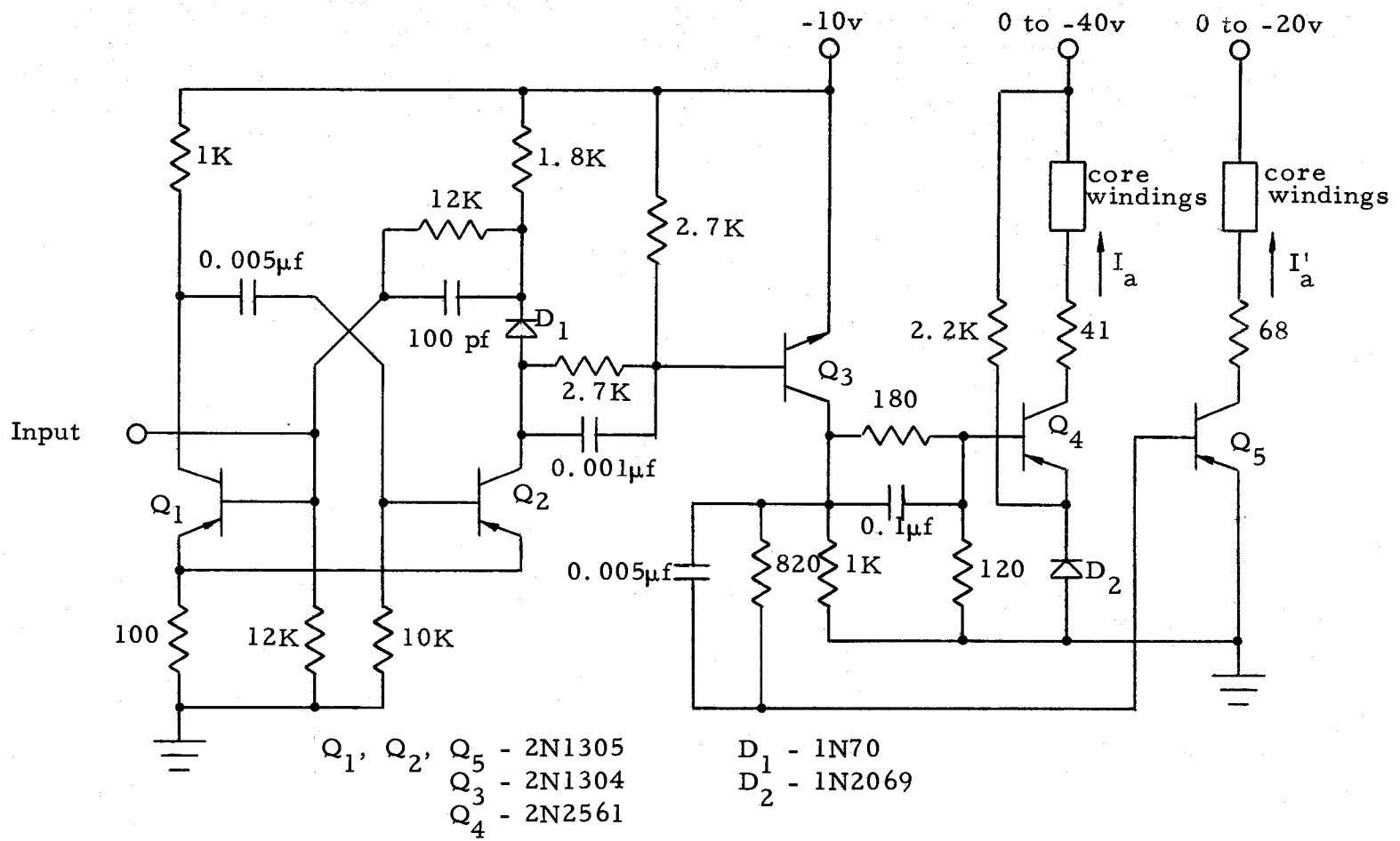

Fig. 29. Circuit diagram of current-pulse generator.

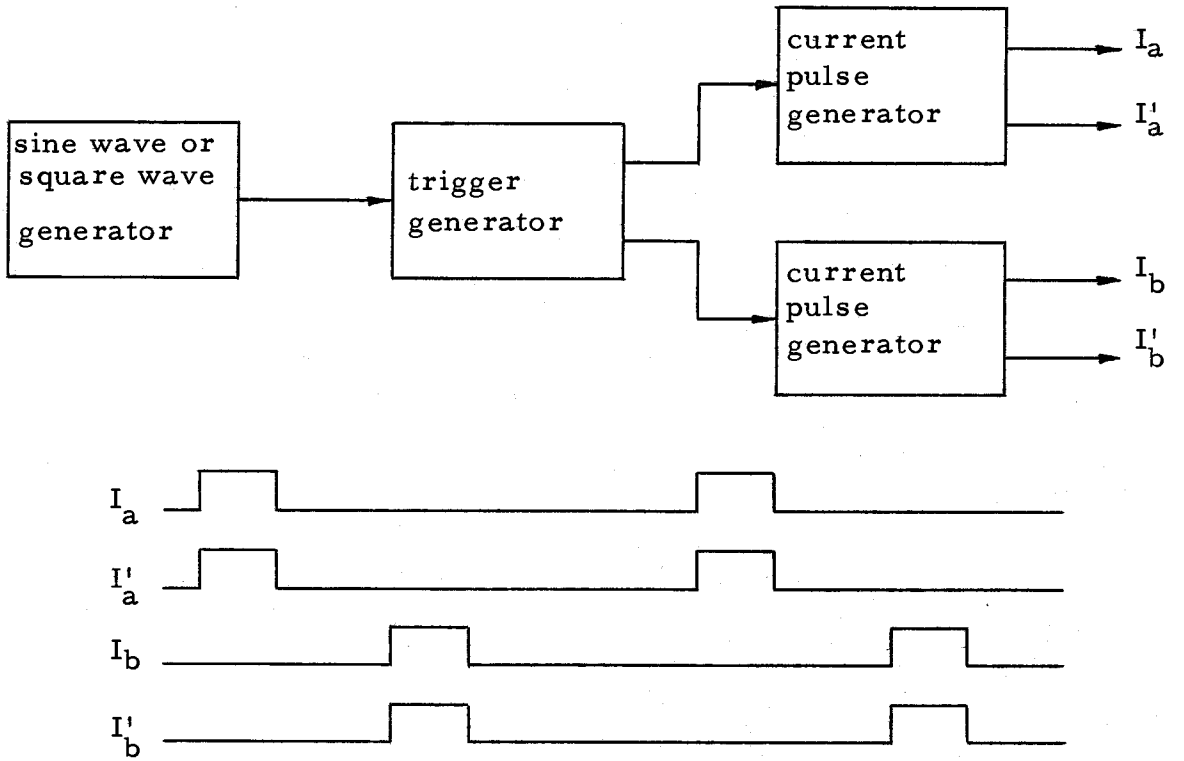

Fig. 30. Block diagram of pulse source and pulse timing.

APPENDIX II

Relative measurements of flux were made with the resistor-capacitor network shown in Fig. 16. In making the measurements, it was assumed that the voltage on the capacitor at time t_2 was linearly related to the area of the input pulse. Upon application of the pulse, the initially discharged capacitor will begin charging; and the voltage e_c across the capacitor at time t_1 will be

$$e_c = E(1-\epsilon^{-t_1/RC}) \tag{37}$$

where R and C are the resistance and capacitance respectively. The capacitor will begin to discharge through the resistor and the pulse source when the input pulse terminates; and because the pulse source is a core winding with negligible resistance, the capacitor discharge will depend on the product of resistance and capacitance. At time t_2 the capacitor voltage will be

$$e_c = E(1-\epsilon^{-t_1/RC})\epsilon^{-(t_2-t_1)/RC} \tag{38}$$

The area of the input pulse is Et_1, and the ratio of the capacitor voltage at time t_2 to the pulse area is

$$K = \frac{(1-\epsilon^{-t_1/RC})\epsilon^{-(t_2-t_1)/RC}}{t_1} \tag{39}$$

The ratio is indeptendent of the pulse amplitude and depends only on the pulse width. The value of K for a pulse width of one microsecond,

which is represented by K_1, was taken as a reference. The percent deviation of K from K_1 is an indication of the error or nonlinearity of the capacitor voltage as a measure of pulse area.

$$\text{Error} = \frac{K_1 - K}{K_1} 100 \tag{40}$$

The error is plotted in Fig. 31 as a function of the input-pulse width. Points for this curve were calculated using values of RC and t_2 of 22 and 15 microseconds respectively.

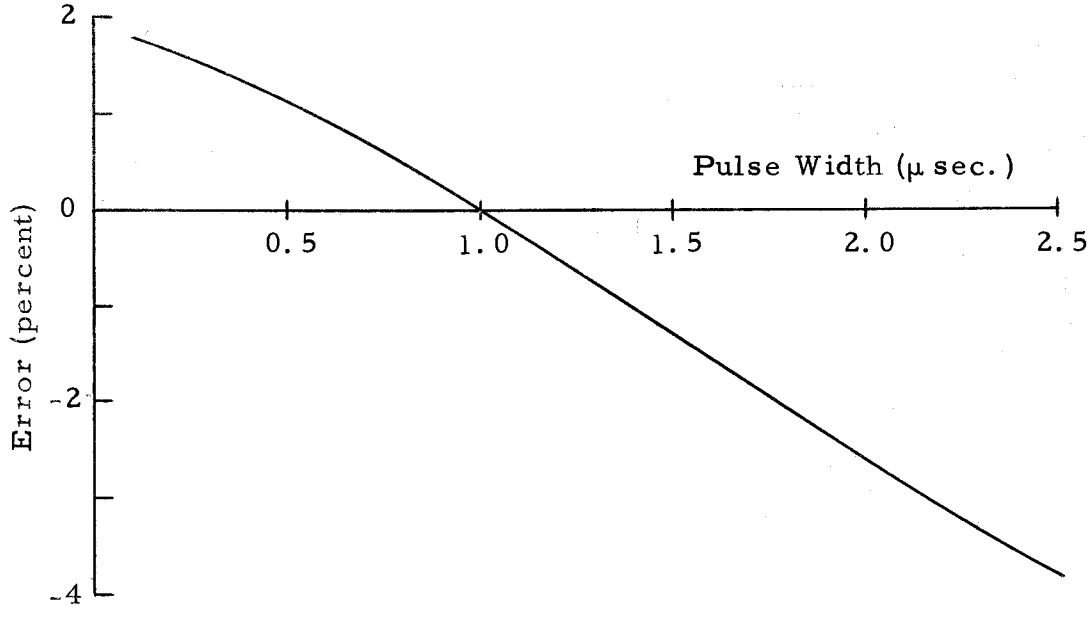

Fig. 31. Error in relative pulse area introduced by resistor-capacitor measurement network.